



A comparison of ASTRAL and RAYMODE propagation loss models and their use in air ASW platforms

Title	A comparison of ASTRAL and RAYMODE propagation loss models and their use in air ASW platforms
Item Type	Thesis
Authors	Huff, Michael Thomas
URI	https://hdl.handle.net/10945/39952
Publisher	Monterey, CA; Naval Postgraduate School
Date Issued	1993-09
Rights	This publication is a work of the U.S. Government as defined in Title 17, United States Code, Section 101. Copyright protection is not available for this work in the United States.
Download date	2026-04-15 00:14:49
Link to Item	https://hdl.handle.net/10945/39952

Downloaded from NPS Archive: Calhoun

**NAVAL POSTGRADUATE SCHOOL
MONTEREY, CALIFORNIA**



THESIS

**A COMPARISON OF ASTRAL AND RAYMODE
PROPAGATION LOSS MODELS AND THEIR USE IN AIR
ASW PLATFORMS**

by

Michael T. Huff

September, 1993

Thesis Advisor:

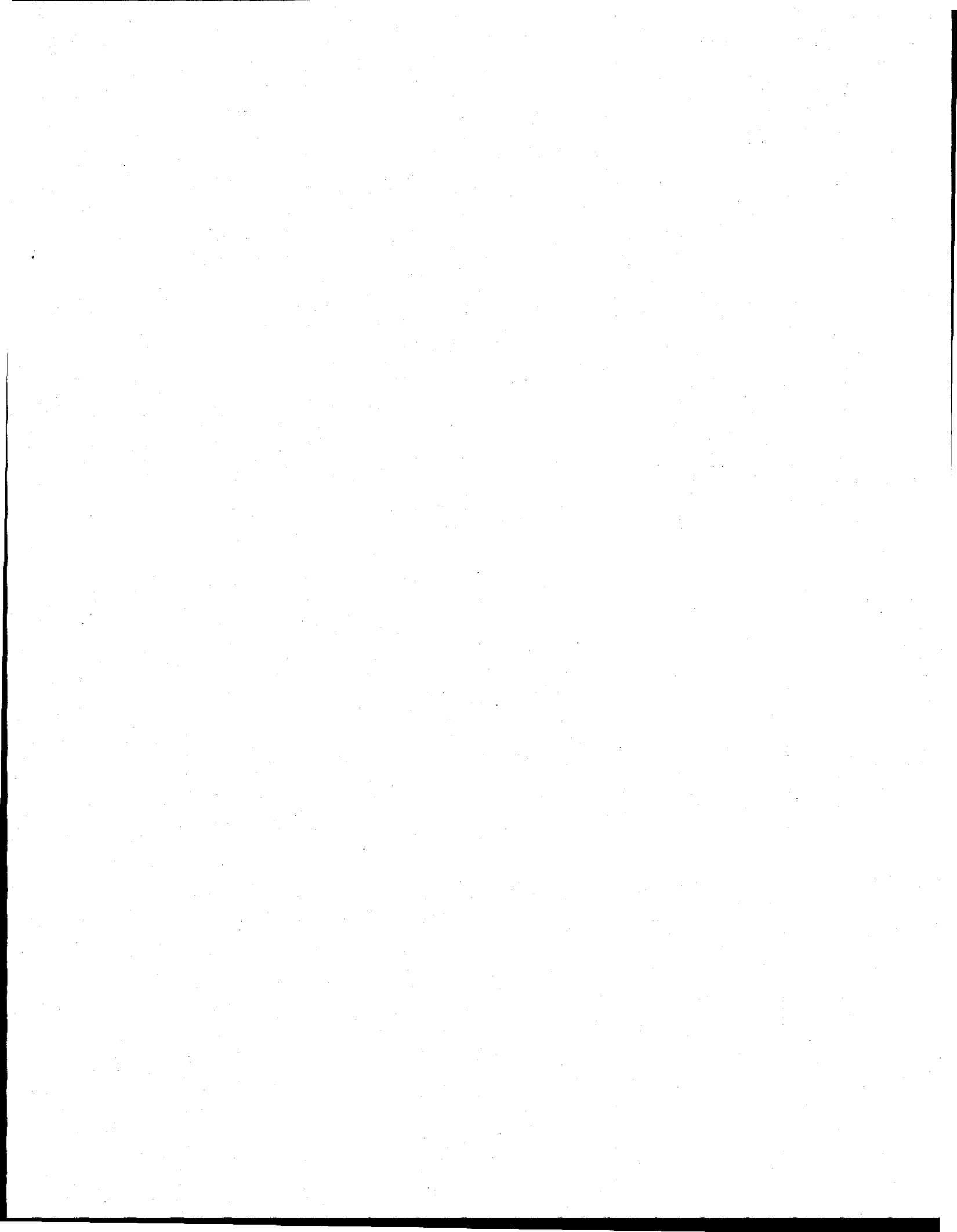
A. B. Coppens

Second Reader:

P. J. Rovero

Approved for public release; distribution is unlimited

Thesis
H85365



REPORT DOCUMENTATION PAGE

Form Approved OMB No. 0704-0188

Public reporting burden for this collection of information is estimated to average 1 hour per response, including the time for reviewing instruction, searching existing data sources, gathering and maintaining the data needed, and completing and reviewing the collection of information. Send comments regarding this burden estimate or any other aspect of this collection of information, including suggestions for reducing this burden, to Washington headquarters Services, Directorate for Information Operations and Reports, 1215 Jefferson Davis Highway, Suite 1204, Arlington, VA 22202-4302, and to the Office of Management and Budget, Paperwork Reduction Project (0704-0188) Washington DC 20503.

1. AGENCY USE ONLY <i>(Leave blank)</i>	2. REPORT DATE September 1993	3. REPORT TYPE AND DATES COVERED Master's Thesis	
4. TITLE AND SUBTITLE A COMPARISON OF ASTRAL AND RAYMODE PROPAGATION LOSS MODELS AND THEIR USE IN AIR ASW PLATFORMS		5. FUNDING NUMBERS	
6. AUTHOR(S) Huff, Michael T.		8. PERFORMING ORGANIZATION REPORT NUMBER:	
7. PERFORMING ORGANIZATION NAME(S) AND ADDRESS(ES) Naval Postgraduate School Monterey CA 93943-5000			
9. SPONSORING/MONITORING AGENCY NAME(S) AND ADDRESS(ES)		10. SPONSORING / MONITORING AGENCY REPORT NUMBER:	
11. SUPPLEMENTARY NOTES The views expressed in this thesis are those of the author and do not reflect the official policy or position of the Department of Defense or the U.S. Government.			
12a. DISTRIBUTION/AVAILABILITY STATEMENT Approved for public release; distribution is unlimited.		12b. DISTRIBUTION CODE	
13. ABSTRACT <i>(maximum 200 words)</i> The development of new decision support systems for Antisubmarine warfare will entail the installation of propagation loss models on ASW aircraft. The decision to put either a range dependent or range independent model in the system will affect the predicted ranges, the overall probability of detection, and the computation time. Comparisons of the range dependent ASTRAL and range independent RAYMODE propagation loss models were made in the Eastern Mediterranean, the Gulf of Oman and the South China Sea for eight source/receiver/frequency combinations. Computation time differences between the two models were not significant at either of the source frequencies (50 Hz or 400 Hz). RAYMODE showed much better correlation with the split step PE model which was used as a standard. The ASTRAL model often predicted lower transmission losses than either RAYMODE or PE. For the short detection ranges normally encountered in air ASW the more complex range dependent models are not necessary. The RAYMODE model or a comparable range independent model will provide adequate propagation loss predictions.			
14. SUBJECT TERMS ASTRAL, RAYMODE, Propagation Loss Models		15. NUMBER OF PAGES: 64	16. PRICE CODE
17. SECURITY CLASSIFICATION OF REPORT Unclassified	18. SECURITY CLASSIFICATION OF THIS PAGE Unclassified	19. SECURITY CLASSIFICATION OF ABSTRACT Unclassified	20. LIMITATION OF ABSTRACT UL

NSN 7540-01-280-5500

Standard Form 298 (Rev. 2-89)
Prescribed by ANSI Std. Z39-18

Approved for public release; distribution is unlimited.

A Comparison of ASTRAL and RAYMODE Propagation Loss Models
and Their Use in Air ASW Platforms

by

Michael Thomas Huff
Lieutenant , United States Navy
B.S., Jacksonville University, 1987


Submitted in partial fulfillment
of the requirements for the degree of

MASTER OF SCIENCE IN APPLIED SCIENCE


from the

NAVAL POSTGRADUATE SCHOOL
September 1993


Author:


Michael Thomas Huff

Approved by:


Alan Coppens, Thesis Advisor


P.J. Rovero, Second Reader


James N. Eagle, Chairman, Antisubmarine Warfare Academic Group

ABSTRACT

The development of new decision support systems for Antisubmarine warfare will entail the installation of propagation loss models on ASW aircraft. The decision to put either a range dependent or range independent model in the system will affect the predicted ranges, the overall probability of detection, and the computation time.

Comparisons of the range dependent ASTRAL and range independent RAYMODE propagation loss models were made in the Eastern Mediterranean, the Gulf of Oman and the South China Sea for eight source/receiver/frequency combinations. Computation time differences between the two models were not significant at either of the source frequencies (50 Hz or 400 Hz). RAYMODE showed much better correlation with the split step PE model which was used as a standard. The ASTRAL model often predicted lower transmission losses than either RAYMODE or PE. For the short detection ranges normally encountered in air ASW the more complex range dependent models are not necessary. The RAYMODE model or a comparable range independent model will provide adequate propagation loss predictions.

Thesis
H85365
C.7

TABLE OF CONTENTS

I. INTRODUCTION	1
II. PROPAGATION LOSS MODELS	3
A. RAYMODE	5
B. ASTRAL	11
III. BACKGROUND	15
A. DESCRIPTION OF AREAS USED	15
B. DATA COLLECTION	19
C. ASSUMPTIONS	21
IV. ANALYSIS	22
A. AREA 1: EASTERN MEDITERRANEAN	22
B. AREA 2: GULF OF OMAN	30
C. AREA 3: SOUTH CHINA SEA	37
V. CONCLUSIONS	44
LIST OF REFERENCES	45
APPENDIX A	46
APPENDIX B	51
INITIAL DISTRIBUTION LIST.	55

LIST OF TABLES

I. Models and Databases Used by ASWTDA.....	20
II. Area 1 Average Predicted Detection Range Differences.....	23
III. Area 2 Average Predicted Detection Range Differences.....	31
IV. Area 3 Average Predicted Detection Range Differences.....	38
V. Area 1 Median Detection Ranges.....	48
VI. Area 2 Median Detection Ranges.....	49
VII. Area 3 Median Detection Ranges.....	50

LIST OF FIGURES

1.	Sonobouy Patterns.....	2
2.	Sound Speed Profile Indicating Criteria for Wavenumber Partitioning.....	8
3.	Location of Area 1 in the Eastern Mediterranean.....	16
4.	Area 1 Sound Speed Profile and Bottom Profile.....	16
5.	Location of Area 2 in the Gulf of Oman.....	17
6.	Area 2 Sound Speed Profile and Bottom Profile.....	17
7.	Location of Area 2 in the South China Sea.....	18
8.	Area 3 Sound Speed Profile and Bottom Profile.....	18
9.	Proploss for Area 1 - 400ft/450ft/400 Hz run (a and b) and 400ft/450ft/50 Hz run (c and d).....	25
10.	Proploss for Area 1 - 400ft/150ft/400 Hz run (a and b) and 400ft/150ft/50 Hz run (c and d).....	26
11.	Proploss for Area 1 - 90ft/450ft/400 Hz run (a and b) and 90ft/450ft/50 Hz run (c and d).....	27
12.	Proploss for Area 1 - 90ft/150ft/400 Hz run (a and b) and 90ft/150ft/50 Hz run (c and d).....	28
13.	Area 1 Cumulative Detection Probabilities, ASTRAL - PE (left) and RAYMODE - PE (right), in Percent(%)	29
14.	Proploss for Area 2 - 400ft/450ft/400 Hz run (a and b) and 400ft/450ft/50 Hz run (c and d).....	32
15.	Proploss for Area 2 - 400ft/150ft/400 Hz run (a and b) and 400ft/150ft/50 Hz run (c and d).....	33
16.	Proploss for Area 2 - 90ft/450ft/400 Hz run (a and b) and 90ft/450ft/50 Hz run (c and d).....	34
17.	Proploss for Area 2 - 90ft/150ft/400 Hz run (a and b) and 90ft/150ft/50 Hz run (c and d).....	35

18. Area 2 Cumulative Detection Probabilities, ASTRAL - PE (left) and RAYMODE - PE (right), in Percent(%)	36
19. Proploss for Area 3 - 400ft/450ft/400 Hz run (a and b) and 400ft/450ft/50 Hz run (c and d).....	39
20. Proploss for Area 3 - 400ft/150ft/400 Hz run (a and b) and 400ft/150ft/50 Hz run (c and d).....	40
21. Proploss for Area 3 - 90ft/450ft/400 Hz run (a and b) and 90ft/450ft/50 Hz run (c and d).....	41
22. Proploss for Area 3 - 90ft/150ft/400 Hz run (a and b) and 90ft/150ft/50 Hz run (c and d).....	42
23. Area 3 Cumulative Detection Probabilities, ASTRAL - PE (left) and RAYMODE - PE (right), in Percent(%).....	43
24. Range Dependent Raytrace with Beamwidth of +/- 20°.....	54
25. Range Dependent Raytrace with Beamwidth of +/- 40°	54

ACKNOWLEDGMENT

The author gratefully acknowledges the help of the following individuals in support of this effort:

Mort Metersky, NAWC - for his help in developing the topic and getting me started

Josh Rovero - for helping to solve most of my computer related questions

Bill Sawrey - whose previous work on ASWTDA helped a great deal

Alan Coppens - for his advice and assistance throughout this project

Les Huff, Senior Acoustic Analyst, GPS Technologies - for being a great role model and good friend

Michelle and Sarah - for their constant support

I. INTRODUCTION

The intent of this paper is to present a comparison study of the effect of using a range dependent versus a range independent propagation loss model in an airborne ASW tactical decision support system. In an ASW tactical situation, processing time and accurate probability of detection are extremely important. The ability to produce quick and reliable transmission loss information while on station would be a definite asset in a decision support role. The two transmission loss models currently being considered as candidates to be installed in an aircraft decision support system are the range dependent ASTRAL or the range independent RAYMODE model [Ref. 1]. Using a range dependent (RD) versus a range independent (RI) propagation loss model may affect both the processing time and the probability of detection.

This study compares the ASTRAL and RAYMODE models in several areas. First, it will review the physics that both models use to develop their propagation loss information. Next, using three different geographical areas and a combination of two source frequencies, two source depths, and two hydrophone depths, transmission loss profiles will be generated. The profiles are then used to develop detection ranges and probabilities of detection for three specific sonobuoy patterns (2x8, 4x4, 5x6x5, shown in Fig. 1, spacing

is based on the predicted detection ranges). The comparisons of the produced transmission loss profiles, the detection ranges, and the probabilities of detection of the patterns will all be presented. The processing time required by each model to run the transmission loss profiles will also be discussed.

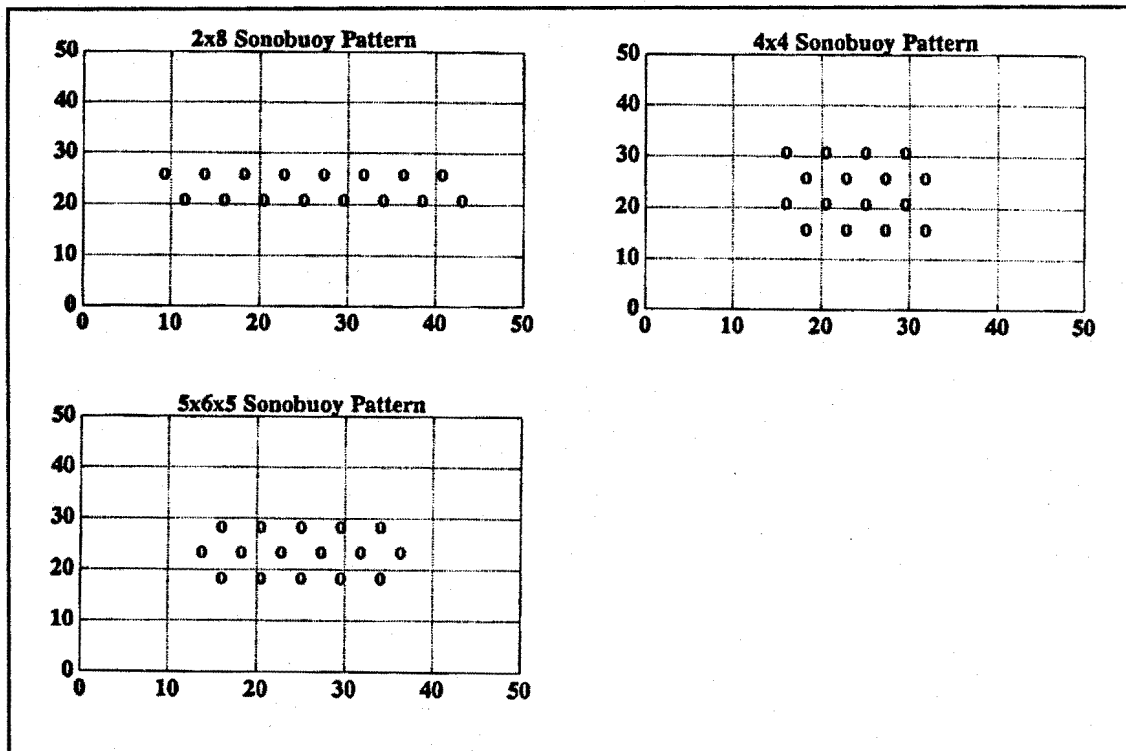


Figure 1 - Sonobuoy Pattern Geometries

II. PROPAGATION LOSS MODELS

The Navy currently uses many different oceanographic and propagation loss models. Propagation loss is the attenuation of the sound intensity as it passes through the ocean from the source to the receiver. Propagation losses are, in general, affected by such factors as the temperature/depth profile of the water column from the surface to the bottom, the source frequency, the condition of the ocean surface (wind speed or sea state), bottom depth, bottom composition and thickness, salinity, source and receiver depths, and range to the source. Once a model is tested and accepted by the Navy it is designated as a Navy Standard Model. There are both range dependent and range independent standard models. The range independent models assume the water column does not change with range and do not take into account the ocean bottom topography. A single sound speed profile, water depth and bottom loss are used for the calculations for an entire area. The range dependent models do use bottom topography and allow the sound speed profile and bottom loss to change with range. RAYMODE is currently the only range independent Navy Standard model, while ASTRAL and PE (Parabolic Equation model) are the most commonly used RD models. The RAYMODE and ASTRAL models use distinctly different methods for calculating the transmission loss from a source to a receiver. In general,

most propagation loss models rely on either wave theory or ray theory [Ref. 2:p. 1].

The wave equation is a partial differential equation relating the acoustic pressure p to the coordinates x, y, z and the time t , and may be written as

$$\frac{\partial^2 p}{\partial t^2} = c^2 \left(\frac{\partial^2 p}{\partial x^2} + \frac{\partial^2 p}{\partial y^2} + \frac{\partial^2 p}{\partial z^2} \right) \quad (1)$$

where c is the sound speed and may vary with the coordinates. There are two basic theoretical approaches to a solution of the wave equation for the specified boundary conditions. The first is *wave theory*, in which the propagation is described in terms of characteristic functions called *normal modes*, each of which is a solution of the wave equation. The normal modes are combined additively to satisfy the source conditions of interest. The result is a complicated mathematical function which, though adequate for computations on a computer, by itself gives little insight on the distribution of the energy of the source in space. The other basic approach to a solution of the wave equation is *ray theory*. The essence of ray theory is that the propagation path of individual rays can be traced by using Snell's Law. The reader interested in an introductory description of wave and ray theory is referred to a book by Officer [Ref. 3]. Snell's Law, one of the most important practical tools of ray theory, describes the refraction of sound rays in a medium of variable sound speed. As applied to an ocean of horizontal layers of isospeed water,

Snell's law states that the grazing angles $\theta_1, \theta_2, \dots$ of a ray at the layer boundaries are related to the sound speeds c_1, c_2, \dots of the layers by

$$\frac{\cos\theta_1}{c_1} = \frac{\cos\theta_2}{c_2} = \frac{\cos\theta_3}{c_3} = \dots = a \text{ constant for any one ray}$$

This expression enables a particular ray to be traced out by following it through the successive layers into which the sound speed profile may have been divided. [Ref. 4]

A. RAYMODE

The passive RAYMODE model predicts the transmission loss of sound through an ocean medium. It is a Navy Standard Passive Acoustic, Range Independent, Propagation Loss Model. The model was developed at the Naval Underwater System Center, New London, by Dr. G.A. Leibiger in 1979 [Ref. 5:p. 1]. RAYMODE has undergone many revisions since it was first presented, but little has been written about the model since 1985. The Navy is currently using Revision 8.1 of the RAYMODE program [Ref. 6:p. iv]. Although the program has been updated to simplify user interface and to utilize new computer technology, the basic physics of the model for calculating propagation losses has changed very little. The RAYMODE model combines the wave and ray theories, described above, using a normal mode summation technique for each propagation path. RAYMODE gives control of many of the propagation loss

variables to the user to provide the most precise definition of the environment. The propagation losses are computed for each path type (e.g., direct path, convergence zone, or bottom bounce), at user-defined ranges and summed for each source angle, or for each of a group of normal modes. The total field at each range is determined by summing the contributions over all path types.

The operation of the RAYMODE model as described by R. C. Medeiros in his overview of the model [Ref. 2:pp. 4-12] is summarized below:

1. The operator is required to provide environmental data and program control parameters, or indicate which historical database to use. These inputs include:

- a. Environmental data:
 - Sound speed versus ocean depth profile
 - Bottom depth
 - Bottom type code (BLUG)
 - Wind speed
- b. Geometrical data:
 - Source depth
 - Receiver depth
- c. Source frequency
- d. Performance data:
 - Minimum and maximum performance ranges
 - Performance range step

2. Input data are processed by the program in preparation for the actual computation and summation of propagation losses.

a. Propagation sound speeds are computed which correspond to the input source and receiver depths by linear interpolation between the entered profile depths. These depths and their associated sound speeds are inserted into the working profile. Together, they define the end-points of the propagation paths.

b. The bottom depth is inserted into the working profile and a corresponding sound speed is extrapolated or interpolated. The profile is then modified by the program to account for the effect of earth curvature.

c. A gradient profile is computed from adjacent values of c as a function of depth. The sound speed gradient, $g = \Delta c / \Delta z$, is the ratio of the change in sound speed and the depth change over which the sound speed change occurs.

d. The profile is thus partitioned into wave number domains, (see Fig. 2) [Ref. 2:p. 5] testing the profile for localized maxima and minima which indicate those water column characteristics, i.e., ducts and layers, that define the propagation paths. The wavenumber

$$\text{wavenumber} = \frac{\text{Frequency}(\text{rad/sec})}{\text{soundspeed}(\text{yard/sec})} \quad (3)$$

is the parameter which most effectively specifies propagation path characteristics such as propagation angles and depths and ranges associated with different propagation modes.

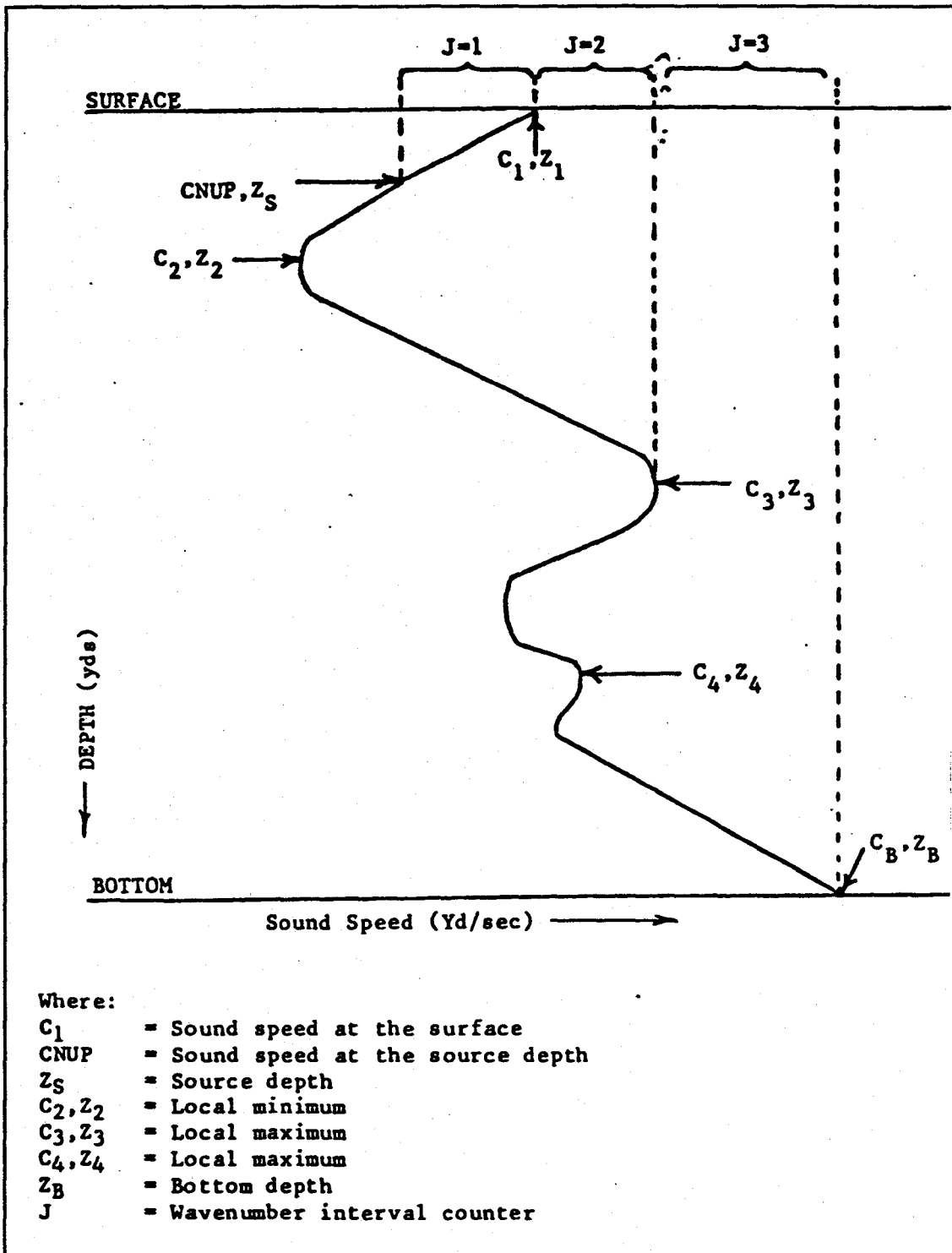


Figure 2 - Sound Speed Profile Indicating Criteria for Wavenumber Partitioning

3. Once these wavenumber domains are determined, they are interpreted by the program as angular intervals, a bounded set of sound propagation angles.

4. For each path, two more quantities are defined. The first is the number of cycles that exist along the path range between the source and receiver. A full cycle is defined as the path from surface or apex to the bottom or nadir and return. A partial cycle is the path from receiver to surface or from the source to surface. The total number of cycles and the partial cycles when appropriately combined yield the path range for a given propagation path. Also a phase change occurs at the turning points which must be accounted for. One additional parameter to be computed is the number of modes which exist for the wavenumber interval under examination. For some paths there may thousands of modes, assuming the frequency is sufficiently high.

When the number of modes propagated in an interval becomes too large, the interval is subdivided into what are called K-regions. A K-region is the interval between two wavenumbers that defines a propagation path. Referring back to Fig. 2, the sound speed profile is partitioned into intervals bounded by a minimum and maximum sound speed. By converting these sound speeds into wavenumbers the interval between the smallest and largest wavenumber is subdivided into a predetermined number of K-region intervals. The K-region

interval is then converted into a propagation angle using Snell's law.

Each K-region interval corresponds to an initial angle of a propagated ray that is extended down the range path with curvature based on the application of Snell's law to the sound speed profile. At each range increment the sum of all the mode contributions from each K-region interval is made resulting in a single combined value of acoustic pressure field. The individual contributions are summed at each range for all the rays in an angular interval, which is then summed to those of previous angular intervals to obtain the total acoustic pressure field at a given range. After correction for boundary losses and sonar beam deviation loss the result is converted to decibels and output as propagation loss versus range. [Ref. 1:pp. 4-6]

When the propagation angle increases, as it does in bottom bounce regions, the number of modes propagated rises, increasing the number of iterations necessary. To avoid this, when the number of modes exceeds 10, the model integrates over a series of K-regions and power sums or coherently sums the contributions of each.

Two types of propagation losses are computed, coherent and random incoherent. Coherent losses are those attributed to ray paths with an exact phase relationship between all paths. Random losses assume a random distribution of phase. Because coherent propagation losses tend to vary widely, small

modifications in input data can cause large changes in output data. The operational RAYMODE model utilizes the random phase propagation loss predictions outputs which tend to be smoothed over the performance range span, providing an expected value of propagation loss. [Ref. 2:p. 12]

B. ASTRAL

ASTRAL (ASEPS Transmission Loss) is a range dependent, low frequency propagation loss model developed by Science Applications International Corporation [Ref. 7:p.ii]. Since ASTRAL'S original version in 1979 it has undergone several modifications. The addition of a surface duct and convergence zone capability has increased its applicability and utility. ASTRAL 4.1 is currently used as one of the Navy Standard Range Dependent Propagation Loss models [Ref. 7:p.3]. The remainder of this section is a summary of the basic physics and theory of the ASTRAL model as described in Refs. 7 and 8.

The calculations in ASTRAL are carried out in two parts, the near field and the far field. The near field calculations are based on a ray trace scheme. The number of rays traced is set to 50 in the operational version. The rays are traced out to a range specified by the user. The angular spread between rays is adjusted so that 80% of the rays have launch angles less than 45 degrees and 20% have launch angles greater than 45 degrees.

In the far field each ray is associated with a set of modes or "smodes". These smodes approximate the envelope of the oscillatory depth function of true normal modes, where pressure can be expressed in the form

$$P = A_1 \sum_n U_n(Z_s) U_n(Z_r) \exp(ik_n r) / \sqrt{K_n r} \quad (4)$$

where Z_s and Z_r are the source and receiver depths respectively. The basic ASTRAL model begins with the normal mode equation [Ref. 7:p. 12]

$$P(r, z) = S_0 k_0^{1/6} \sum_n U_n(z) U_n(Z_0) \exp(ik_n r) \quad (5)$$

where S_0 is a constant related to the source strength divided by the square root of the range r , the U are normalized depth functions, k_0 is a reference wave number (equal to $2\pi f/c_0$, where c_0 is a reference sound speed), and the asymptotic form has been used for the Hankel function. The symbol i is the square root of minus one. The intensity is assumed to be in the form

$$I = A_2 \sum_n Y_n^2(z_s) Y_n^2(z_r) / k_0 \quad (6)$$

where

$$Y_n^2(z) = [r_c(\theta_n) \tan \theta_n(z)]^{-1} \quad (7)$$

and where $r_c(\theta_n)$ is the apex-to-apex cycle range of a ray launched with angle θ_n . The summation over modes is replaced by a summation over sets of modes, so Equation 4 can be written as

$$I = A_3 \sum_m Y_m^2(z_s) Y_m^2(z_r) X_m, \quad (8)$$

where each value of the running index corresponds to a set of modes, or "smodes." The variable X_m is given by N_m/k_o , where N_m is the number of modes in the smode. In the ASTRAL code, these average values are actually calculated at specific ray angles measured relative to the axis of minimum sound speed and thus a smode corresponds to an angle bin. Using the phase integral ψ_m , where

$$\psi_m = \int [\sin(\theta_m(z))/c(z)] dz \quad (9)$$

then $N_m = \omega_m \psi_m / \pi$. If $\psi_m / (\sin\theta\delta\theta)$ is assumed constant, then the pressure can be expressed as

$$P = \sum_m y_m(z_s) y_m(z_r) X_m k_o^{-1/2} \quad (10)$$

where

$$y_m(z) \rightarrow \sqrt{Y_m^2(z)} \quad (11)$$

and

$$X_m = \cos[\omega_o \psi_m(z_s)] \cos[\omega_o \psi_m(z_r)] \exp(ik_m r). \quad (12)$$

The smode is then extended at the turning points via Airy functions. The smodes are propagated in the far field until an environmental change occurs. If the structure of the

sound-speed field changes then a new smode assignment must be made using the new turning point structure and assuming adiabatic invariance. As the environment changes, the phase integral is kept constant by choosing a new turning point sound speed. [Ref. 8]

Convergence zone effects can be added if each smode is assumed to be composed of four parts that correspond to the four different up/down arrivals at both source and receiver. Each of the components is propagated in range using the cycle length of the smode and the intensity of each is assumed to be proportional to the square of a $\sin(x)/x$ function. At each range the intensity is summed and smoothed.[Ref. 8] The full derivation of this concept is beyond the scope of this paper. For a full description of Convergence Zone ASTRAL the reader is referred to Ref. 7, pp. 14-18.

III. BACKGROUND

A. DESCRIPTION OF AREAS USED

Three areas were chosen for the ASTRAL and RAYMODE comparisons. The areas were chosen based on the new regionally focused Navy strategy stated in "From the Sea...". The specific coordinates for the areas investigated were picked at random and then rounded to the nearest degree for ease of data entry. Each of the three areas are 50 nm by 50 nm boxes.

The first area is in the Eastern Mediterranean centered at 33N/033E. Area 1, located between Egypt and Cyprus as shown in Fig. 3, is typical of one in which an air ASW platform might have to search for a third world submarine. The area is close enough to the coast to be considered littoral but too deep to really be considered shallow water. The bottom contour and sound speed profile are shown in Fig 4. The surface temperature in the area is 60° F , there is a layer depth of 350 ft, the depth excess is 525 fms and there is a sound channel at 715 ft.

Area 2 in the Gulf of Oman, is centered on 24-30N/059E. This region has become a fairly high interest area since the Persian Gulf War. The specific area used for the study is shown in Fig. 5. The sound speed profile for the center of

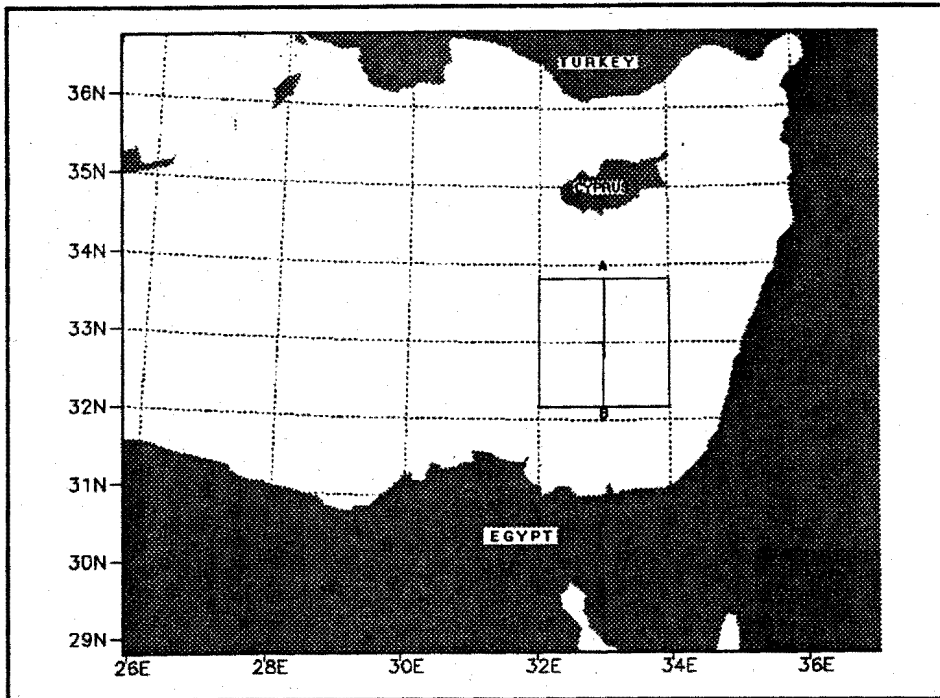


Figure 3 - Location of Area 1 in Eastern Mediterranean

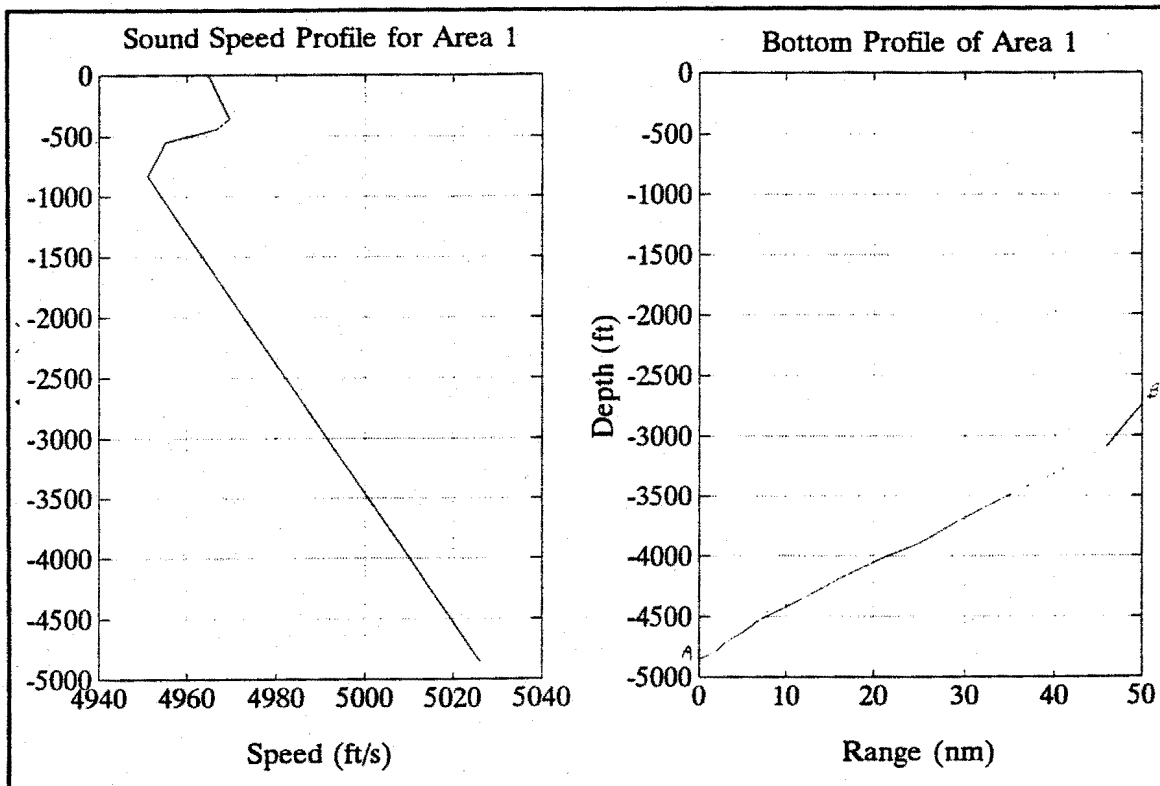


Figure 4 - Sound Speed Profile and Bottom Profile for Area 1

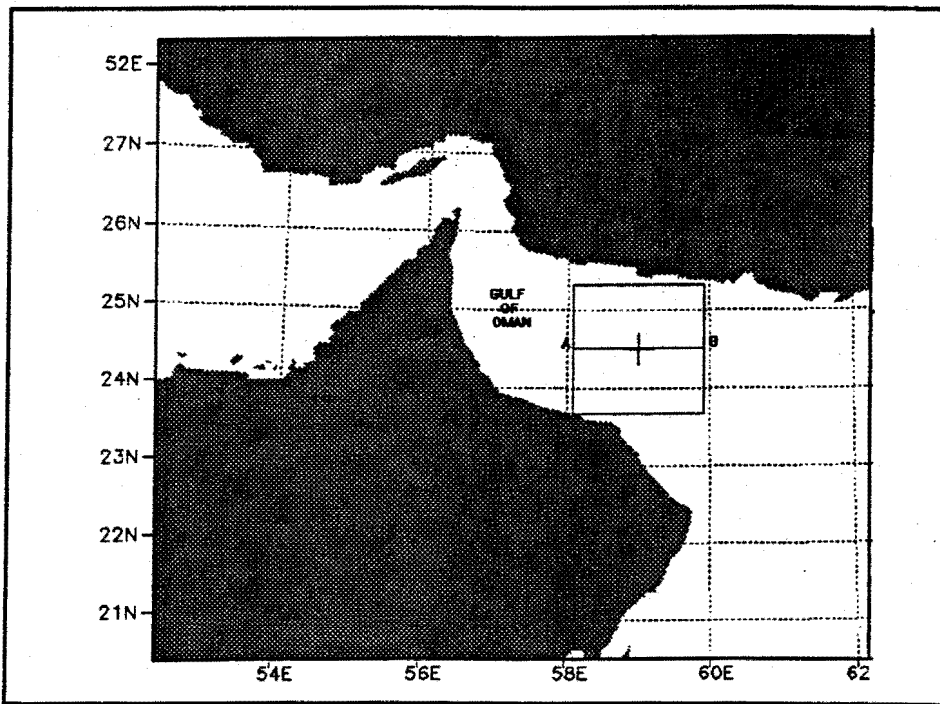


Figure 5 - Location of Area 2 in Gulf of Oman

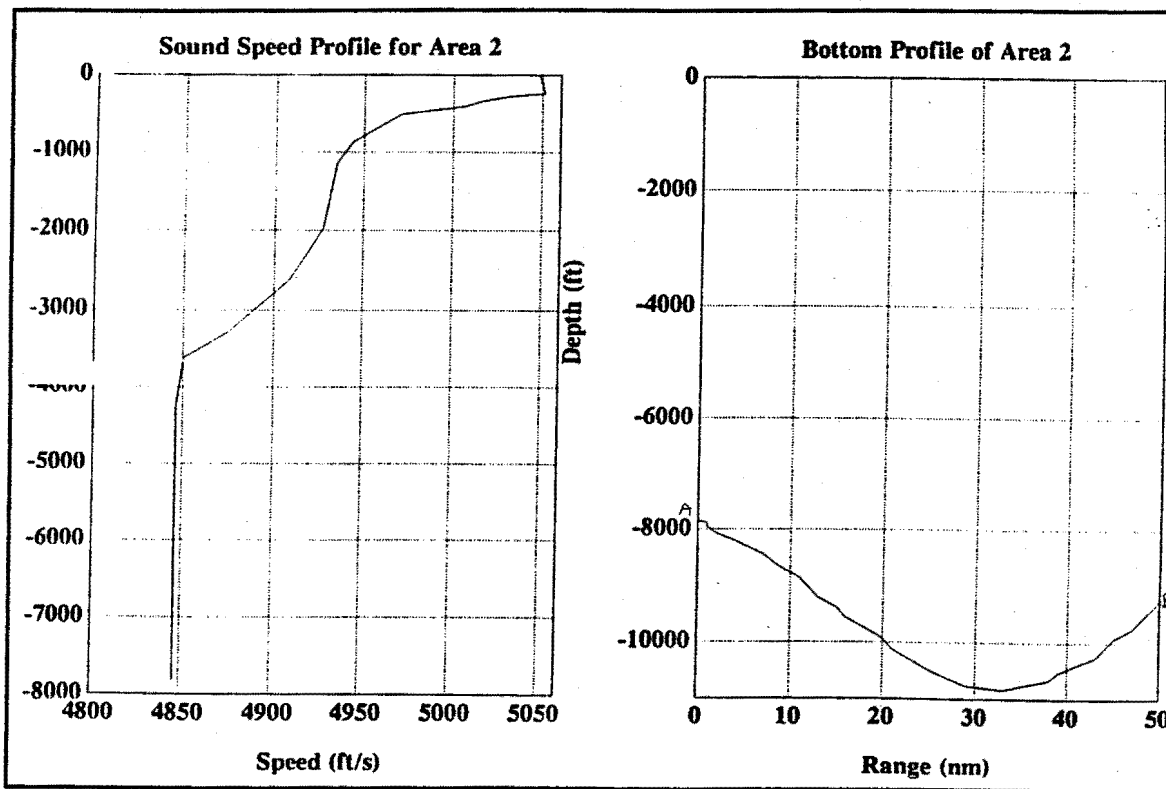


Figure 6 - Sound Speed Profile and Bottom Profile for Area 2

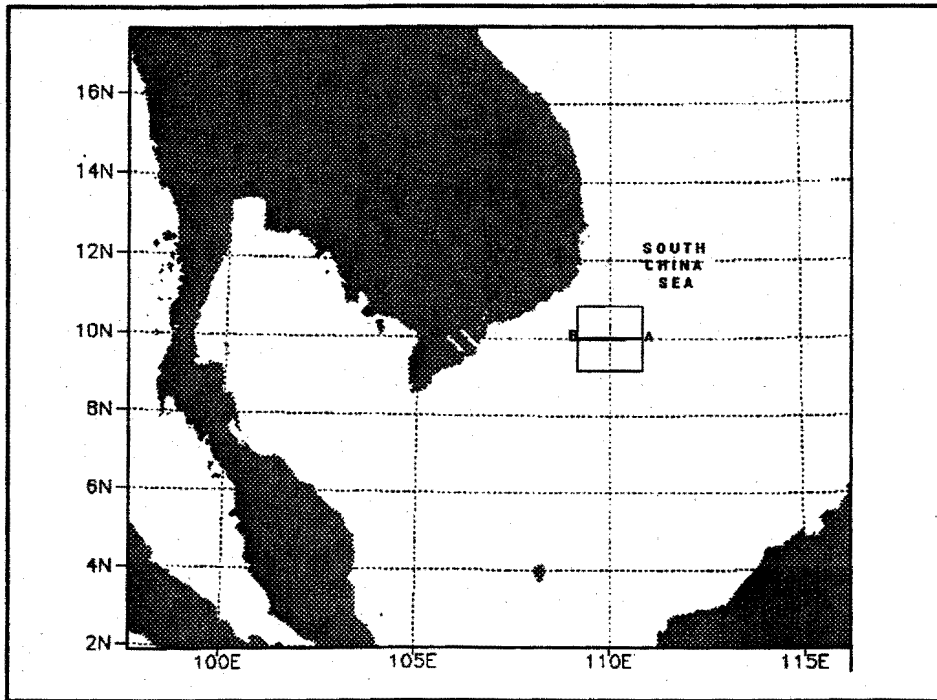


Figure 7 - Location of Area 3 in South China Sea

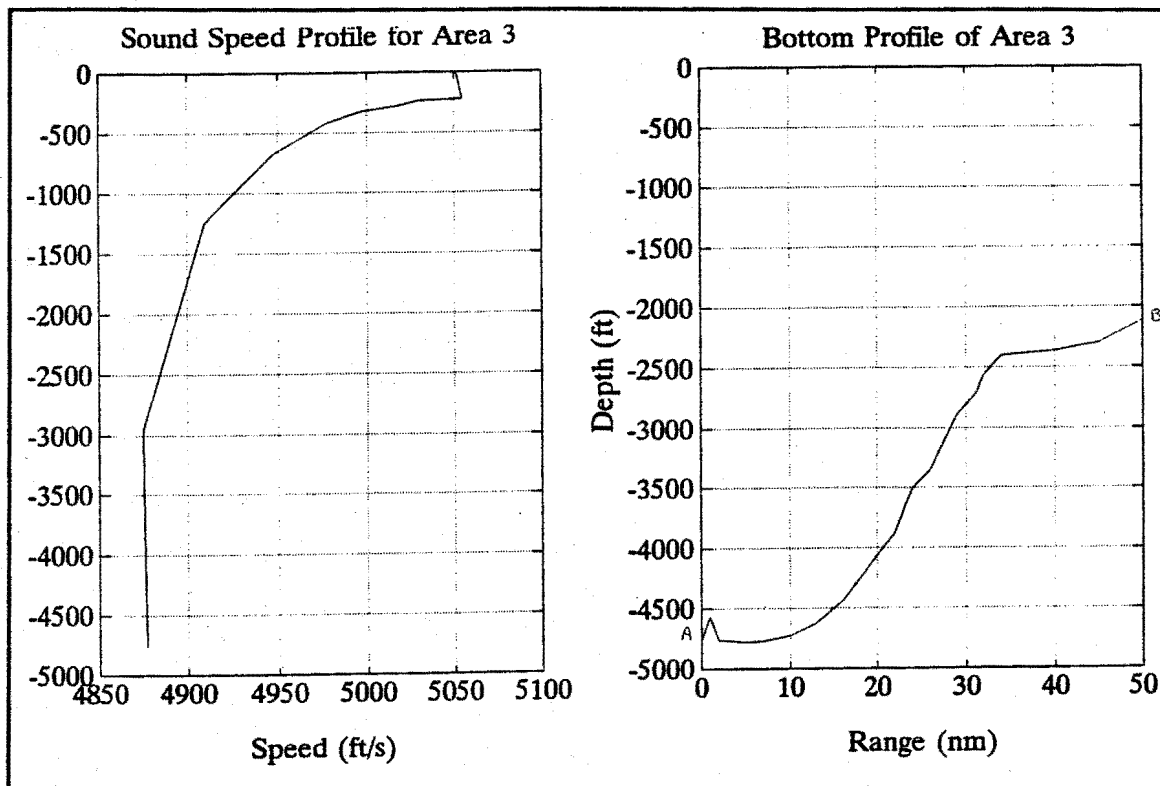


Figure 8 - Sound Speed Profile and Bottom Profile for Area 3

the area, and the bottom profile are shown in Fig. 6. A surface temperature of 80° F results in a large negative gradient below the layer depth of 250 ft. There is no depth excess (depth needed for convergence zone propagation to exist) in this area and the sound channel is fairly deep at approximately 4000 ft.

The third area is in the South China Sea at 10N/110E, only 75 miles off the coast of Vietnam (Fig. 7). The sound speed profile is similar to the one in Area 2 with a strong negative gradient below the layer (Fig. 8). The surface temperature is 75° F, and the sound channel is at 2000 ft. Similar to Area 2, there is no depth excess.

B. DATA COLLECTION

The ASTRAL, RAYMODE, and PE models used for this study were run inside a new developmental ASW Tactical Decision Aid (ASWTDA version 2.1.2.1) which has many ASW tactical applications. The ASWTDA program is run on a SUN work station. The databases used by ASWTDA are the Oceanographic and Atmospheric Master Library (OAML) and the GEM database. The GEM database is a subset of OAML and was created by ASWTDA's developing contractor, SONALYSTS, Inc., in order to reduce the OAML database size and the time required to access the information. Table I lists the versions of the models and databases used by ASWTDA. [Ref. 9]

Database or Model	ASWTDA (V.2.1.2.1)
LFBL	2.0
HFBL	2.0
DBDBC	1.0
GDEM	3.0
GEM	1.0
SHIP NOISE	4.0
SEDIMENT	3.0
PASSIVE RAYMODE	8.1
PE	3.0
CZ ASTRAL	2.4

Table I - Models and Databases Used by ASWTDA

LFBL and HFBL are low and high frequency bottom loss databases, GDEM is an oceanographic environmental database and DBDBC is the bathymetry database. The areas of interest were generated inside ASWTDA's "Environmental" function with 20 sample points inside each 50 nm by 50 nm box. Propagation loss profiles were generated for the combinations of 90 and 400 ft receivers, 150 and 450 ft depth targets, and 50 and 400 Hz sources. This produced 8 range dependent and 8 range independent profiles for each area. The specific technique and code used to extract this data is shown in Section B of Appendix A. The propagation loss profiles were then evaluated using a Matlab subroutine to produce Median Detection Ranges (MDR) for Figures of Merit (FOM's) of 65, 70, 75, and 80 dB. Three distributive sonobuoy patterns (4x4, 5x6x5, 2x8) were evaluated at each FOM and receiver/source/frequency

combination. A pattern evaluation program provided by Wagner Associates called NESST was used to produce probabilities of detection for the three selected patterns. A description of the NESST program and how the CDP's were obtained is included in Appendix B.

C. ASSUMPTIONS

For the purpose of this study several basic assumptions were made. The first is that the split-step PE propagation loss model is sufficiently accurate to serve as the basis for comparisons. The target, for the probability of detection calculations, is assumed to be uniformly distributed in a 50 nm by 50 nm box. In most littoral ASW situations the passive detection ranges are relatively short (1 to 10 nm). Therefore, even though the data for the entire area was used for analysis purposes, the profiles generated were only graphed out to 30 nm. The sonobuoys were considered to be cookie cutter detectors: if the target was inside the given range of the specific sonobuoy it was counted as a detection and if it was outside the range it was considered as undetected.

IV. ANALYSIS

A. AREA 1: EASTERN MEDITERRANEAN

Figures 9-12 compare the ASTRAL and RAYMODE propagation loss profiles against PE generated profiles. Analysis of the ASTRAL profiles shows much lower dB loss versus range than in the PE model or the losses expected from spherical spreading. (The "x" marks on the graphs indicate spherical spreading at 1, 2, and 3 nm.) The RAYMODE profiles correlate very well with the spherical spreading and the PE profiles, with the exception of the 90ft/150ft/400 Hz run. This lack of correlation in the shallow/shallow situation is most likely due to the fact that both the source and receiver are in the mixed layer and the 400 Hz source frequency is above the 150 Hz cutoff frequency for a layer of that depth. The RAYMODE model does not predict the surface duct and therefore gives much shorter predicted ranges.

Predicted detection ranges were obtained from the proploss profiles by extracting the range at which the profile crossed the given figure of merit. The ranges for each FOM are tabulated in Appendix A. The average differences in the detection ranges are shown in Table II.

The calculated detection ranges were used to construct the three sonobuoy patterns, with a buoy spacing of 1.5 MDR

ASTRAL - PE

Run	FOM 65
A1MMH	0.2
A1MML	0.3
A1MSH	0.2
A1MSL	0.4
A1SMH	0.4
A1SML	0.5
A1SSH	-0.2
A1SSL	0.6
AVG DIF	0.3

RAYMODE - PE

FOM 65
-0.3
-0.2
-0.2
-0.1
-0.3
-0.3
-1.1
-0.3
-0.3

ASTRAL - RAYMODE

FOM 65
0.5
0.5
0.4
0.5
0.7
0.7
0.9
0.9
0.6

ASTRAL - PE

Run	FOM 70
A1MMH	0.8
A1MML	1.8
A1MSH	0.5
A1MSL	1.4
A1SMH	1.0
A1SML	1.4
A1SSH	-0.2
A1SSL	1.4
AVG DIF	1.0

RAYMODE - PE

FOM 70
-0.5
-0.3
-0.7
-0.7
-0.7
-0.6
-4.2
-1.0
-1.1

ASTRAL - RAYMODE

FOM 70
1.3
2.1
1.2
2.1
1.7
2.0
4.0
2.4
2.1

ASTRAL - PE

Run	FOM 75
A1MMH	3.0
A1MML	3.9
A1MSH	2.0
A1MSL	2.9
A1SMH	2.6
A1SML	4.9
A1SSH	-1.6
A1SSL	7.1
AVG DIF	3.1

RAYMODE - PE

FOM 75
0.3
0.2
-0.7
1.1
-0.8
-2.0
-11.8
0.0
-1.7

ASTRAL - RAYMODE

FOM 75
2.7
3.7
2.7
1.8
3.4
6.9
10.2
7.1
4.8

ASTRAL - PE

Run	FOM 80
A1MMH	0.4
A1MML	14.5
A1MSH	1.1
A1MSL	4.2
A1SMH	1.5
A1SML	10.0
A1SSH	16.4
A1SSL	5.6
AVG DIF	6.7

RAYMODE - PE

FOM 80
-5.3
1.5
-8.7
-0.1
-8.3
1.1
-10.0
-2.8
-4.1

ASTRAL - RAYMODE

FOM 80
5.7
13.0
9.8
4.3
9.8
8.9
26.4
8.4
10.8

Table II - Area 1 Average Predicted Detection Range Differences

and a row spacing of 1.67 MDR as prescribed in the ASW tactical manuals. The pattern in each scenario that generated the largest cumulative detection probability (CDP) was used in Fig. 13 to compare the CDP's of each model. (The first column in the table is the run ID which is described in more detail in Appendix A.) It should be noted that in the case of RAYMODE vs PE (Fig. 14) at an FOM of 70 the average difference not including the A1SSH run is only 4.0%. At FOM's of 65 and 70 dB the average difference in detection probability when compared to PE is fairly close. At an FOM of 75 dB however, ASTRAL vs PE has an average difference of 45.1% while RAYMODE vs PE is only 7.9%. The ranges at an FOM of 80 dB were in excess of 15 nm and resulted in CDP's of 100 percent in all three models with the exception of the cross layer high frequency scenarios in the RAYMODE model. (The 80 FOM results were not included in CDP comparisons for Area 1.)

No appreciable difference in computation time between ASTRAL and RAYMODE was found using a source frequency of either 50 or 400 Hz. Typically both models required approximately 3 to 5 seconds to generate proploss curves at 50 Hz. At 400 Hz the ASTRAL model took an average of 2 seconds longer to generate the propagation loss curve than the RAYMODE model which generally took 5 sec.

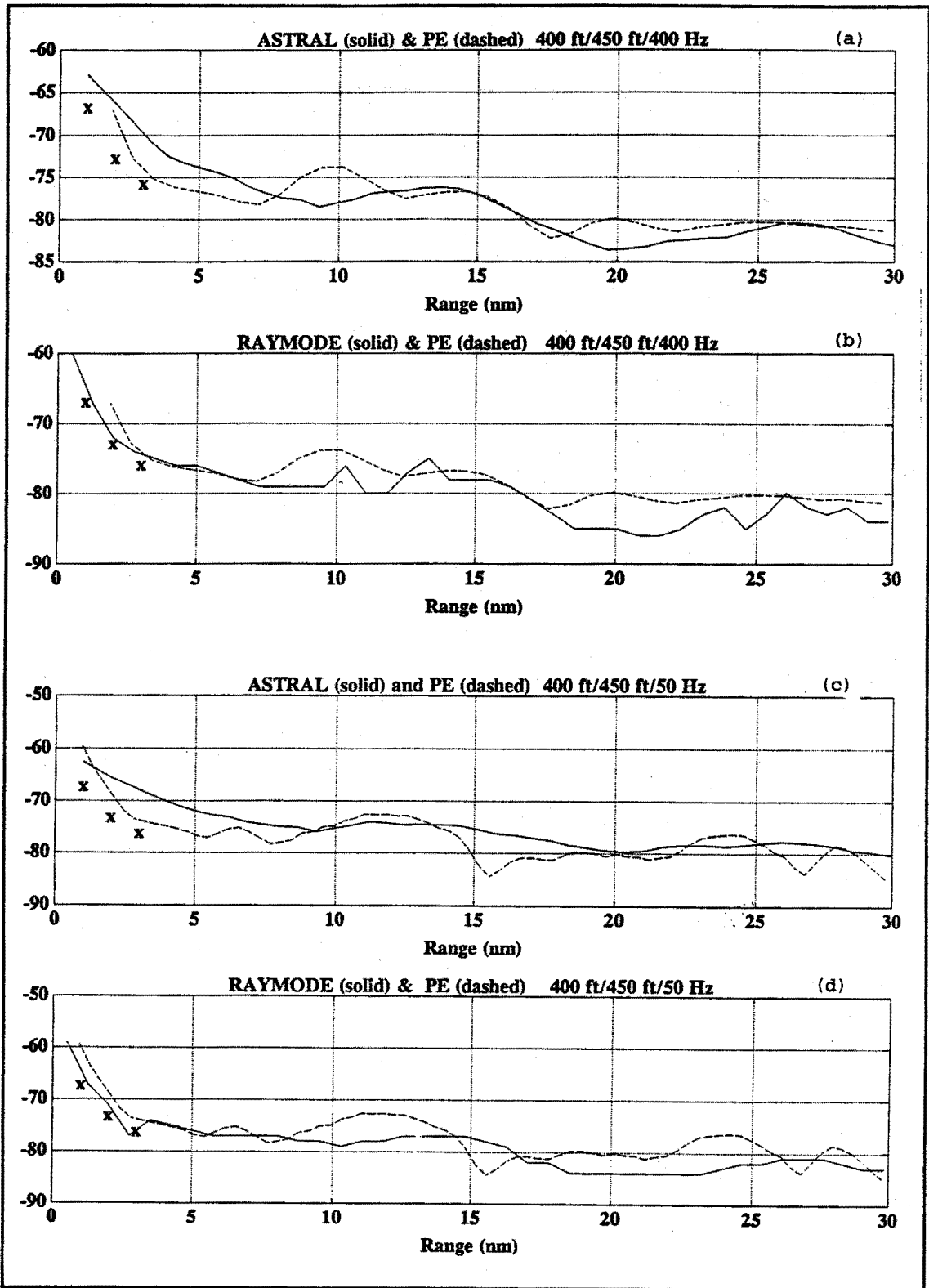


Figure 9 - Proploss for Area 1: 400ft/450ft/400 Hz (a and b)
400ft/450ft/50 Hz (c and d)

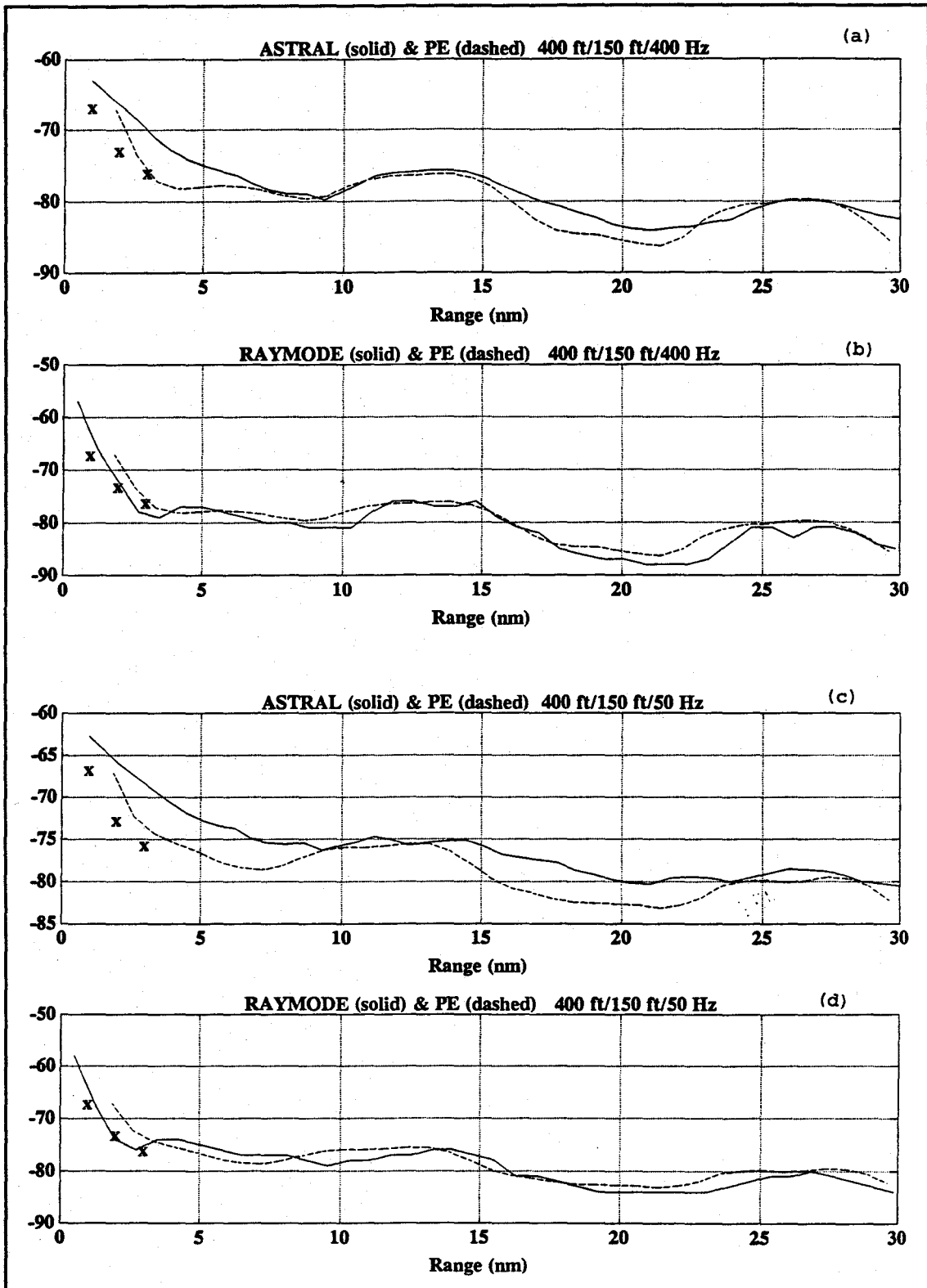


Figure 10 - Proploss for Area 1: 400ft/150ft/400 Hz (a and b), 400ft/150ft/50 Hz (c and d)

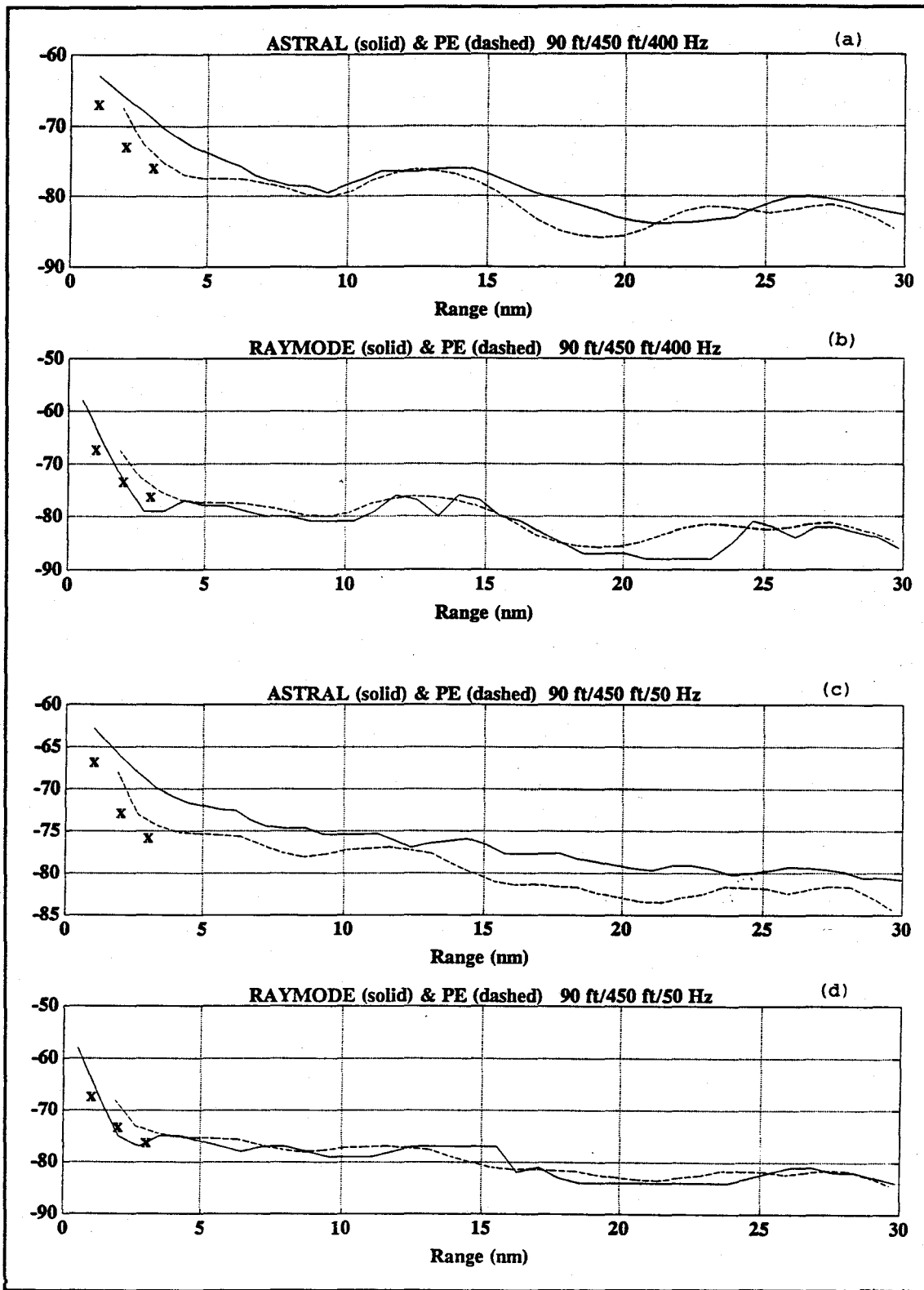


Figure 11 - Proploss for Area 1: 90ft/450ft/400 Hz (a and b), 90ft/450ft/50 Hz (c and d)

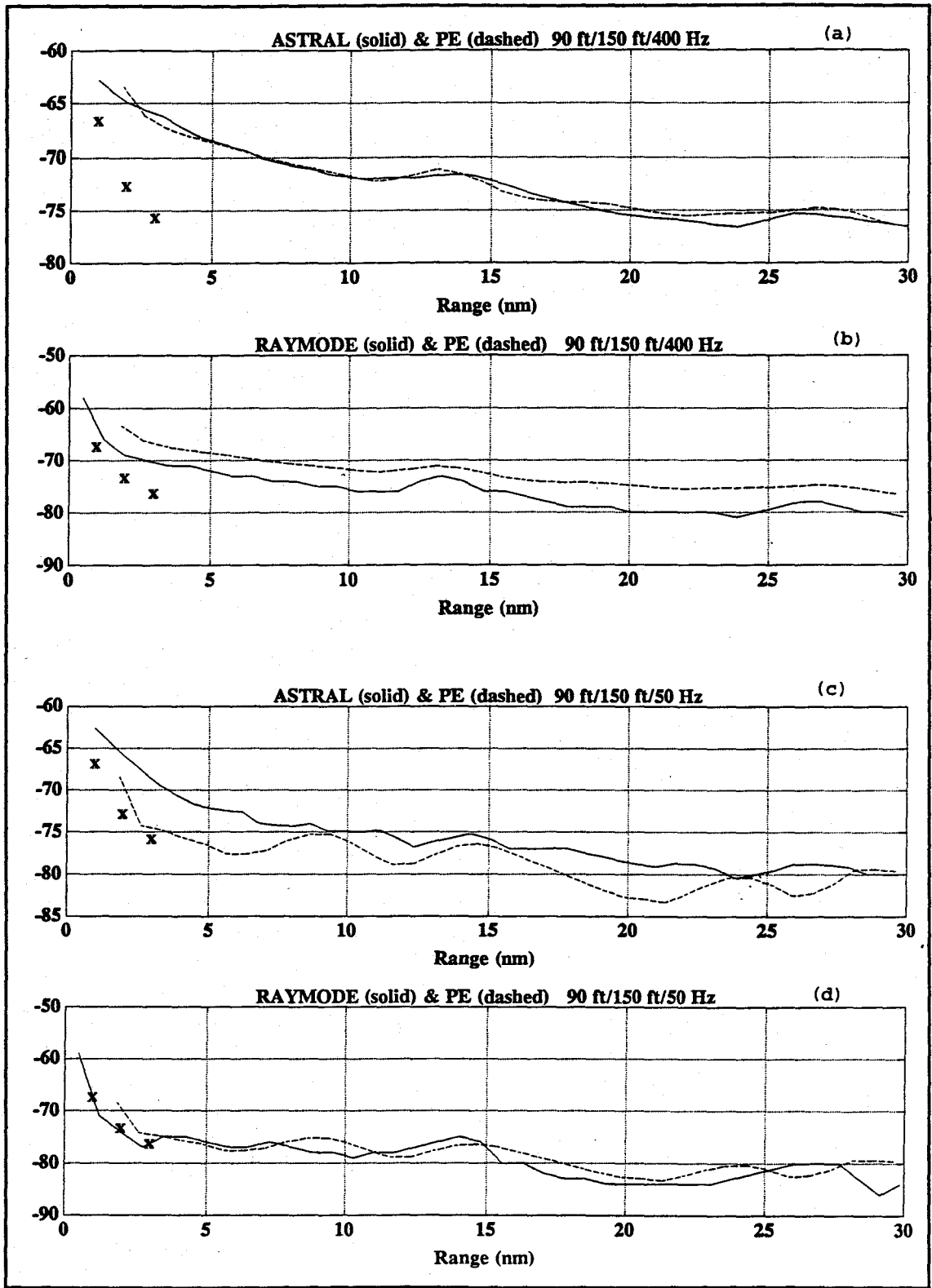


Figure 12 - Proploss for Area 1: 90ft/150ft/400 Hz (a and b), 90ft/150ft/50 Hz (c and d)

FOM 65			
Run	ASTRAL	PE	DIFF
A1MMH	4.3	3.1	1.2
A1MML	4.8	3.1	1.7
A1MSH	4.8	3.5	1.3
A1MSL	5.1	3.1	2.0
A1SMH	4.8	2.5	2.3
A1SML	4.8	2.4	2.4
A1SSH	7.8	9.6	-1.8
A1SSL	6.2	3.1	3.1
Avg diff			2.0

FOM 65			
Run	RAY	PE	DIFF
A1MMH	1.9	3.1	-1.2
A1MML	2.4	3.1	-0.7
A1MSH	2.5	3.5	-1.0
A1MSL	2.5	3.1	-0.6
A1SMH	1.4	2.5	-1.1
A1SML	1.2	2.4	-1.2
A1SSH	2.5	9.6	-7.1
A1SSL	1.9	3.1	-1.2
Avg diff			-1.8

FOM 70			
Run	ASTRAL	PE	DIFF
A1MMH	16.8	8.7	8.1
A1MML	25.2	7.7	17.5
A1MSH	14.0	9.6	4.4
A1MSL	23.1	8.7	14.4
A1SMH	19.2	9.6	9.6
A1SML	20.4	7.7	12.7
A1SSH	75.4	82.3	-6.9
A1SSL	20.4	7.7	12.7
Avg diff			10.8

FOM 70			
Run	RAY	PE	DIFF
A1MMH	5.1	8.7	-3.6
A1MML	5.8	7.7	-1.9
A1MSH	4.8	9.6	-4.8
A1MSL	4.3	8.7	-4.4
A1SMH	4.8	9.6	-4.8
A1SML	4.3	7.7	-3.4
A1SSH	14.0	82.3	-68.3
A1SSL	2.4	7.7	-5.3
Avg diff			-12.1

FOM 75			
Run	ASTRAL	PE	DIFF
A1MMH	65.3	17.2	48.1
A1MML	94.1	30.1	64.0
A1MSH	27.8	16.8	11.0
A1MSL	75.4	25.2	50.2
A1SMH	55.7	17.0	38.7
A1SML	98.1	28.6	69.5
A1SSH	100.0	100.0	0.0
A1SSL	100.0	20.4	79.6
Avg diff			45.1

FOM 75			
Run	RAY	PE	DIFF
A1MMH	19.5	17.2	2.3
A1MML	32.1	30.1	2.0
A1MSH	8.8	16.8	-8.0
A1MSL	42.1	25.2	16.9
A1SMH	8.8	17.0	-8.2
A1SML	6.8	28.6	-21.8
A1SSH	96.8	100.0	-3.2
A1SSL	19.5	20.4	-0.9
Avg diff			7.9

Figure 13 - Cumulative Detection Probability Comparisons (%)
 ASTRAL-PE (left) and RAYMODE-PE (right)

B. AREA 2: GULF OF OMAN

The transmission losses in Area 2 were much greater than in Area 1. The propagation loss profiles in Figs. 14-17 show a greater than 80dB loss in less than five miles in all but the 90ft/150ft/400 Hz case. The rapid loss of sound energy in such a short range resulted in a much higher correlation between all three models. (The cyclical appearance of the 50 Hz PE proploss profiles, seen here in Area 2 and even more apparent in Area 3, is examined further in Appendix B). The average differences in the predicted median detection ranges are shown in Table III. ASTRAL consistently predicts longer ranges than PE, while RAYMODE generally predicts ranges shorter than PE.

The small differences in ranges similarly resulted in CDP differences (Fig. 18) usually less than 10%. Just as in Area 1 computations, no significant difference in the computation time between ASTRAL and RAYMODE was noted.

ASTRAL - PE	
Run	FOM 65
A2MMH	0.3
A2MML	-0.1
A2MSH	0.5
A2MSL	0.2
A2SMH	0.2
A2SML	0.1
A2SSH	-0.1
A2SSL	0.2
AVG DIF	0.2

RAYMODE - PE	
	FOM 65
	-0.5
	-0.3
	-0.6
	-0.6
	-0.6
	-0.6
	-0.5
	0.7
	-0.4

ASTRAL - RAYMODE	
	FOM 65
	0.8
	0.2
	1.1
	0.8
	0.8
	0.7
	0.4
	-0.5
	0.5

Run	FOM 70
A2MMH	0.7
A2MML	0.4
A2MSH	0.8
A2MSL	0.4
A2SMH	0.2
A2SML	0.3
A2SSH	0.0
A2SSL	0.4
AVG DIF	0.4

	FOM 70
	-0.1
	-0.6
	-0.4
	-0.9
	-0.9
	-0.9
	-1.1
	0.9
	-0.5

	FOM 70
	0.8
	1.0
	1.2
	1.3
	1.1
	1.2
	1.1
	-0.5
	0.9

Run	FOM 75
A2MMH	1.2
A2MML	0.9
A2MSH	1.2
A2MSL	1.0
A2SMH	1.0
A2SML	0.9
A2SSH	-0.4
A2SSL	0.9
AVG DIF	0.8

	FOM 75
	-0.3
	-0.8
	-0.3
	-0.6
	-0.8
	-0.8
	-0.2
	2.7
	-0.1

	FOM 75
	1.5
	1.7
	1.5
	1.6
	1.8
	1.7
	-0.2
	-1.8
	1.2

Run	FOM 80
A2MMH	1.6
A2MML	1.3
A2MSH	2.0
A2MSL	0.9
A2SMH	2.1
A2SML	0.8
A2SSH	-1.9
A2SSL	0.9
AVG DIF	1.0

	FOM 80
	-0.2
	-1.0
	-1.0
	-1.3
	-1.4
	-1.5
	2.5
	2.2
	-0.2

	FOM 80
	1.8
	2.3
	3.0
	2.2
	3.5
	2.3
	-4.4
	-1.3
	1.2

Table III - Area 2 Average Predicted Detection Range Differences

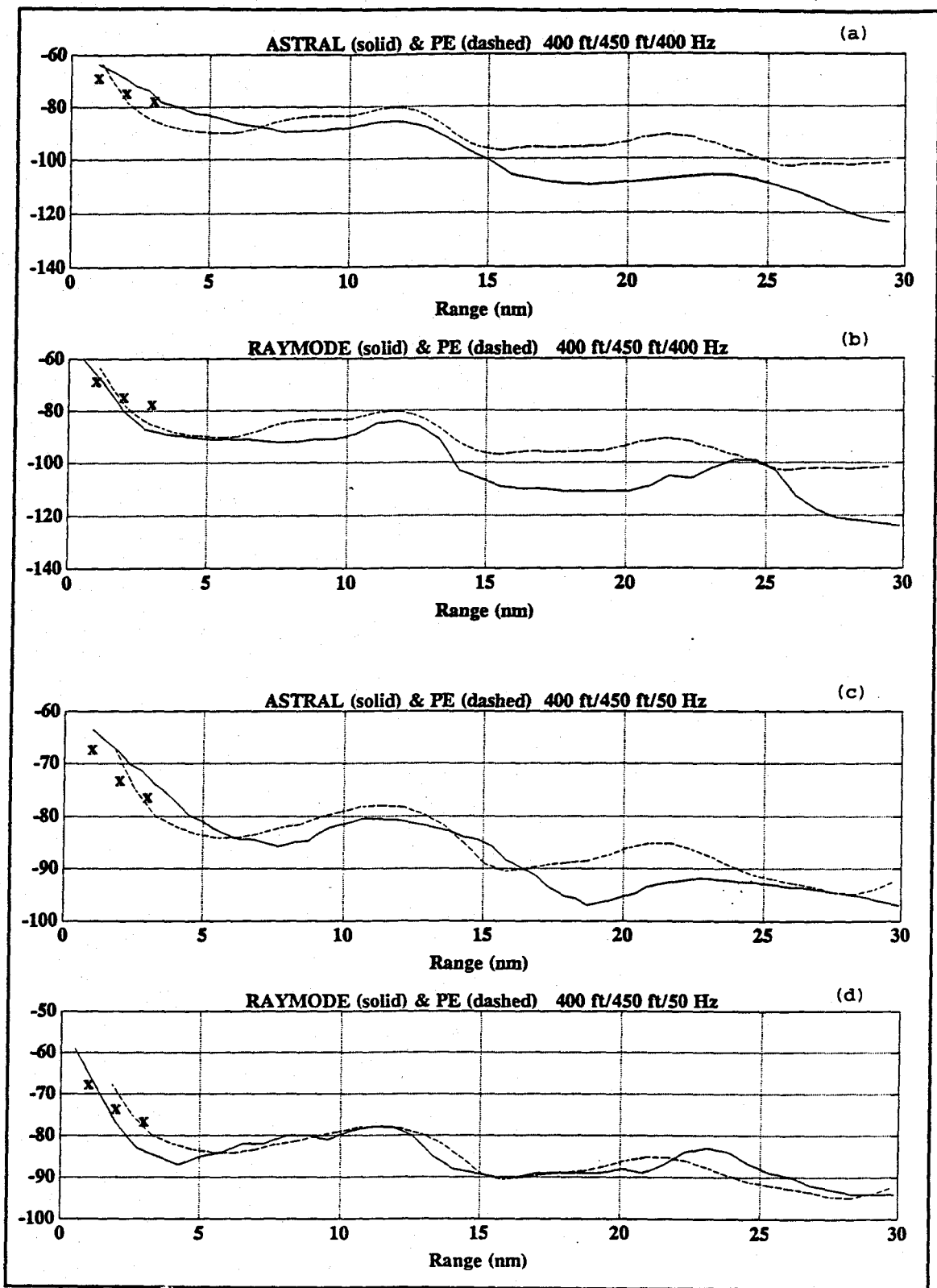


Figure 14 - Proploss for Area 2: 400ft/450ft/400 Hz (a and b), 400ft/450ft/50 Hz (c and d)

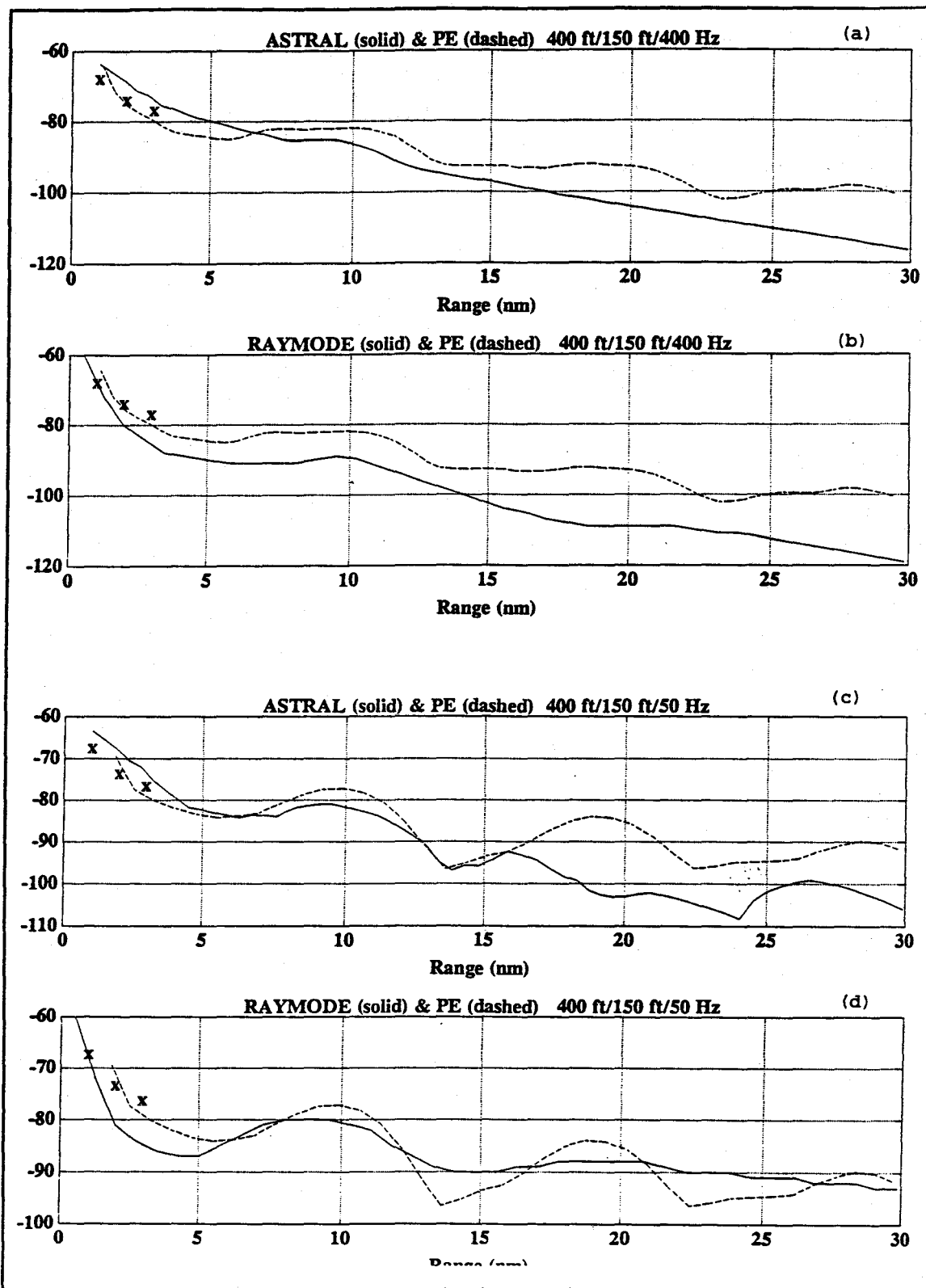


Figure 15 - Proploss for Area 2: 400ft/150ft/400 Hz (a and b), 400ft/150ft/50 Hz (c and d)

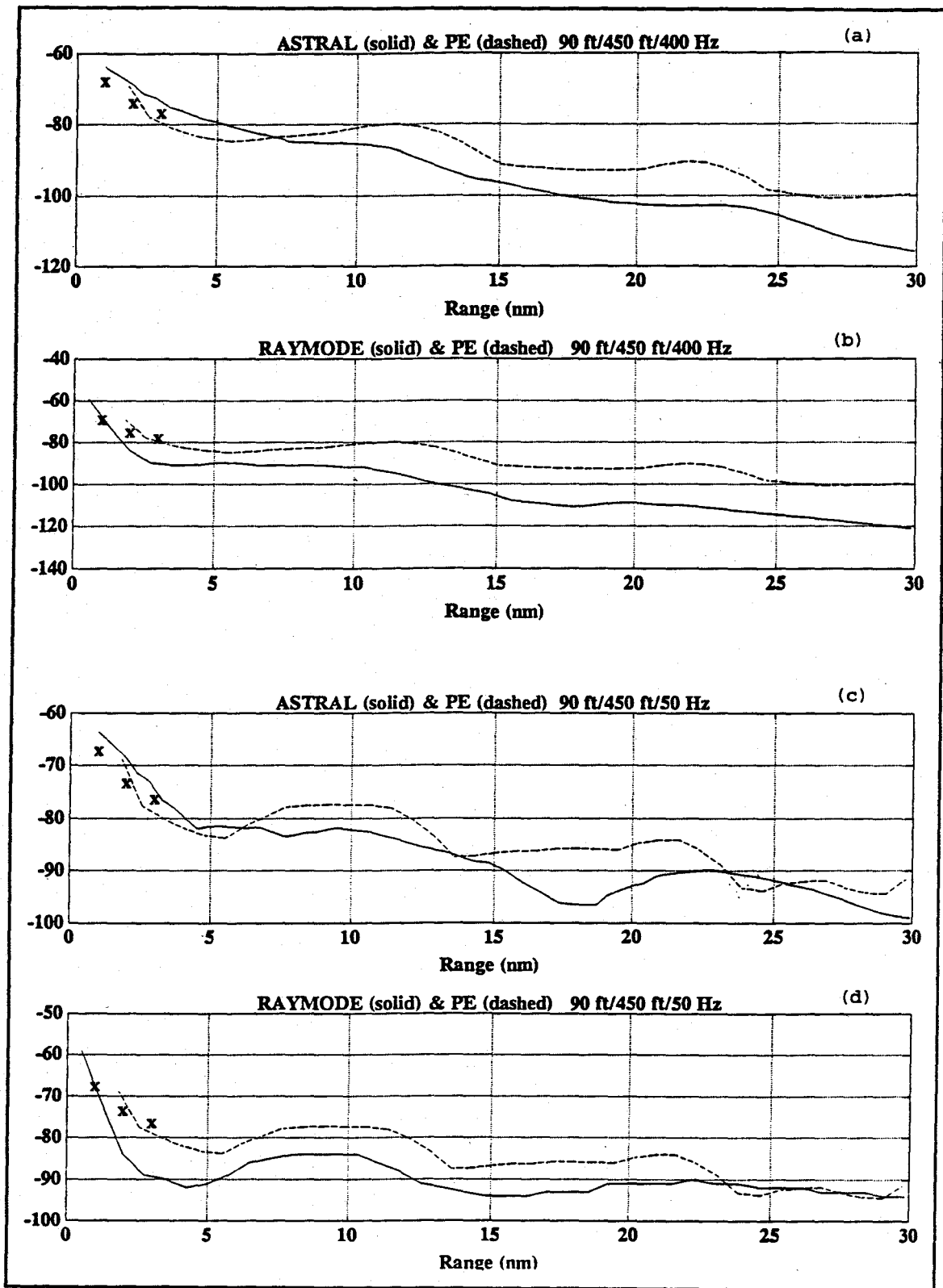


Figure 16 - Proploss for Area 2: 90ft/450ft/400 Hz (a and b), 90ft/450ft/50 Hz (c and d)

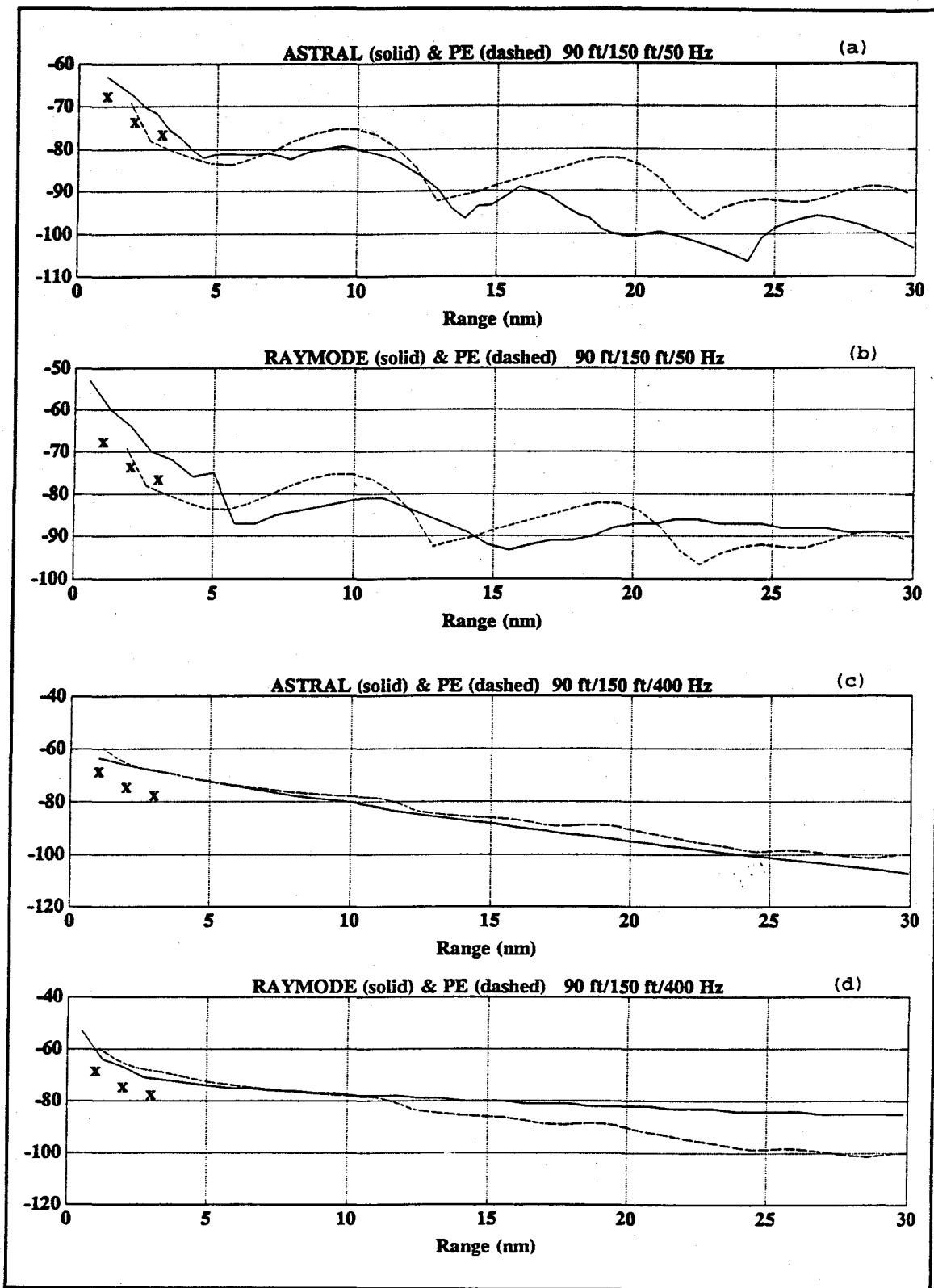


Figure 17 - Proploss for Area 2: 90ft/150ft/400 Hz
(a and b), 90ft/150ft/50 Hz (c and d)

FOM 65			
Run	ASTRAL	PE	DIFF
A2MMH	4.3	2.5	1.8
A2MML	3.1	3.5	-0.4
A2MSH	5.1	2.5	2.6
A2MSL	4.3	3.1	1.2
A2SMH	4.3	3.1	1.2
A2SML	3.5	3.1	0.4
A2SSH	6.0	6.2	-0.2
A2SSL	4.8	3.5	1.3
Avg diff			1.1

FOM 65			
Run	RAY	PE	DIFF
A2MMH	1.0	2.5	-1.5
A2MML	2.4	3.5	-1.1
A2MSH	1.0	2.5	-1.5
A2MSL	1.0	3.1	-2.1
A2SMH	1.0	3.1	-2.1
A2SML	1.0	3.1	-2.1
A2SSH	3.5	6.2	-2.7
A2SSL	7.7	3.5	4.2
Avg diff			2.2

FOM 70			
Run	ASTRAL	PE	DIFF
A2MMH	7.7	3.5	4.2
A2MML	10.7	6.8	3.9
A2MSH	8.7	3.5	5.2
A2MSL	9.6	6.2	3.4
A2SMH	7.7	6.2	1.5
A2SML	8.1	6.2	1.9
A2SSH	24.8	24.8	0.0
A2SSL	9.6	6.2	3.4
Avg diff			2.9

FOM 70			
Run	RAY	PE	DIFF
A2MMH	3.1	3.5	-0.4
A2MML	3.5	6.8	-3.3
A2MSH	1.9	3.5	-1.6
A2MSL	1.9	6.2	-4.3
A2SMH	1.9	6.2	-4.3
A2SML	1.9	6.2	-4.3
A2SSH	12.1	24.8	-12.7
A2SSL	14.0	6.2	7.8
Avg diff			4.8

FOM 75			
Run	ASTRAL	PE	DIFF
A2MMH	16.8	5.8	11.0
A2MML	20.4	11.4	9.0
A2MSH	17.0	6.2	10.8
A2MSL	17.2	8.7	8.5
A2SMH	17.2	8.7	8.5
A2SML	17.0	8.7	8.3
A2SSH	67.9	74.3	-6.4
A2SSL	17.2	9.6	7.6
Avg diff			8.8

FOM 75			
Run	RAY	PE	DIFF
A2MMH	4.3	5.8	-1.5
A2MML	5.8	11.4	-5.6
A2MSH	4.8	6.2	-1.4
A2MSL	4.8	8.7	-3.9
A2SMH	3.5	8.7	-5.2
A2SML	3.5	8.7	-5.2
A2SSH	71.6	74.3	-2.7
A2SSL	42.1	9.6	32.5
Avg diff			7.3

FOM 80			
Run	ASTRAL	PE	DIFF
A2MMH	24.8	8.7	16.1
A2MML	36.5	19.2	17.3
A2MSH	42.1	16.8	25.3
A2MSL	30.4	17.2	13.2
A2SMH	49.3	17.2	32.1
A2SML	30.4	19.2	11.2
A2SSH	98.6	100.0	-1.4
A2SSL	30.4	17.2	13.2
Avg diff			16.2

FOM 80			
Run	RAY	PE	DIFF
A2MMH	6.8	8.7	-1.9
A2MML	8.8	19.2	-10.4
A2MSH	6.8	16.8	-10.0
A2MSL	6.2	17.2	-11.0
A2SMH	5.8	17.2	-11.4
A2SML	5.8	19.2	-13.4
A2SSH	100.0	100.0	0.0
A2SSL	50.0	17.2	32.8
Avg diff			11.4

Figure 18 - Cumulative Detection Probability Comparisons (%)
 ASTRAL-PE (left) and RAYMODE-PE (right)

C. AREA 3: SOUTH CHINA SEA

The propagation loss profiles in Area 3 (Figs. 19-22) showed very large variations. In the first two scenarios ASTRAL and RAYMODE predict ranges two times greater than those generated from PE for a FOM of 70 dB. At an FOM of 75 dB the ranges are as much as five times greater. Even though both models differ greatly from PE the correlation between ASTRAL and RAYMODE is better than in areas 1 and 2. In the 400 Hz runs the RAYMODE and ASTRAL profiles have a much higher agreement with PE than in the 50 Hz runs. The average differences for just the 50 Hz runs for ASTRAL vs PE and RAYMODE vs PE, at an FOM of 70, are 2.1 nm and 2.3 nm respectively. For the 400 Hz runs the differences are only 1.1 and .55 nm respectively. Similar relationships are true for the other FOM's as well. The reason for this is not exactly known. The overall differences in ranges are shown in Table IV.

The differences between the detection probabilities (Fig. 23) for all three models appear to be similar in this area. Approximately 2% at FOM of 65 dB, and 13% at FOM of 70 dB. The big difference in this area is that correlation between ASTRAL and RAYMODE is better overall than either ASTRAL to PE or RAYMODE to PE.

ASTRAL - PE	
Run	FOM 65
A3MMH	0.6
A3MML	0.6
A3MSH	0.7
A3MSL	0.7
A3SMH	0.2
A3SML	0.4
A3SSH	0.0
A3SSL	0.7
AVG DIF	0.5

RAYMODE - PE	
	FOM 65
	0.0
	1.0
	-0.1
	0.4
	0.0
	0.5
	0.1
	0.9
	0.4

ASTRAL - RAYMODE	
	FOM 65
	0.6
	-0.4
	0.8
	0.3
	0.2
	-0.1
	-0.1
	-0.2
	0.1

ASTRAL - PE	
Run	FOM 70
A3MMH	1.2
A3MML	1.6
A3MSH	1.4
A3MSL	1.7
A3SMH	1.7
A3SML	1.9
A3SSH	-0.1
A3SSL	3.1
AVG DIF	1.6

RAYMODE - PE	
	FOM 70
	1.5
	3.4
	0.1
	2.0
	0.3
	2.2
	-0.3
	1.7
	1.4

ASTRAL - RAYMODE	
	FOM 70
	-0.3
	-1.8
	1.3
	-0.3
	1.4
	-0.3
	0.2
	1.4
	0.2

ASTRAL - PE	
Run	FOM 75
A3MMH	1.9
A3MML	6.7
A3MSH	2.5
A3MSL	4.9
A3SMH	3.1
A3SML	4.6
A3SSH	0.8
A3SSL	5.9
AVG DIF	3.8

RAYMODE - PE	
	FOM 75
	3.8
	8.0
	0.3
	4.1
	0.7
	4.5
	-0.8
	3.6
	3.0

ASTRAL - RAYMODE	
	FOM 75
	-1.9
	-1.3
	2.2
	0.8
	2.4
	0.1
	1.6
	2.3
	0.8

ASTRAL - PE	
Run	FOM 80
A3MMH	7.2
A3MML	9.4
A3MSH	1.8
A3MSL	9.2
A3SMH	0.7
A3SML	5.2
A3SSH	-0.5
A3SSL	10.1
AVG DIF	5.4

RAYMODE - PE	
	FOM 80
	5.5
	11.0
	-1.4
	6.8
	-2.3
	4.0
	0.4
	2.1
	3.3

ASTRAL - RAYMODE	
	FOM 80
	1.7
	-1.6
	3.2
	2.4
	3.0
	1.2
	-0.9
	8.0
	2.1

Table IV - Area 3 Average Predicted Detection Range Differences

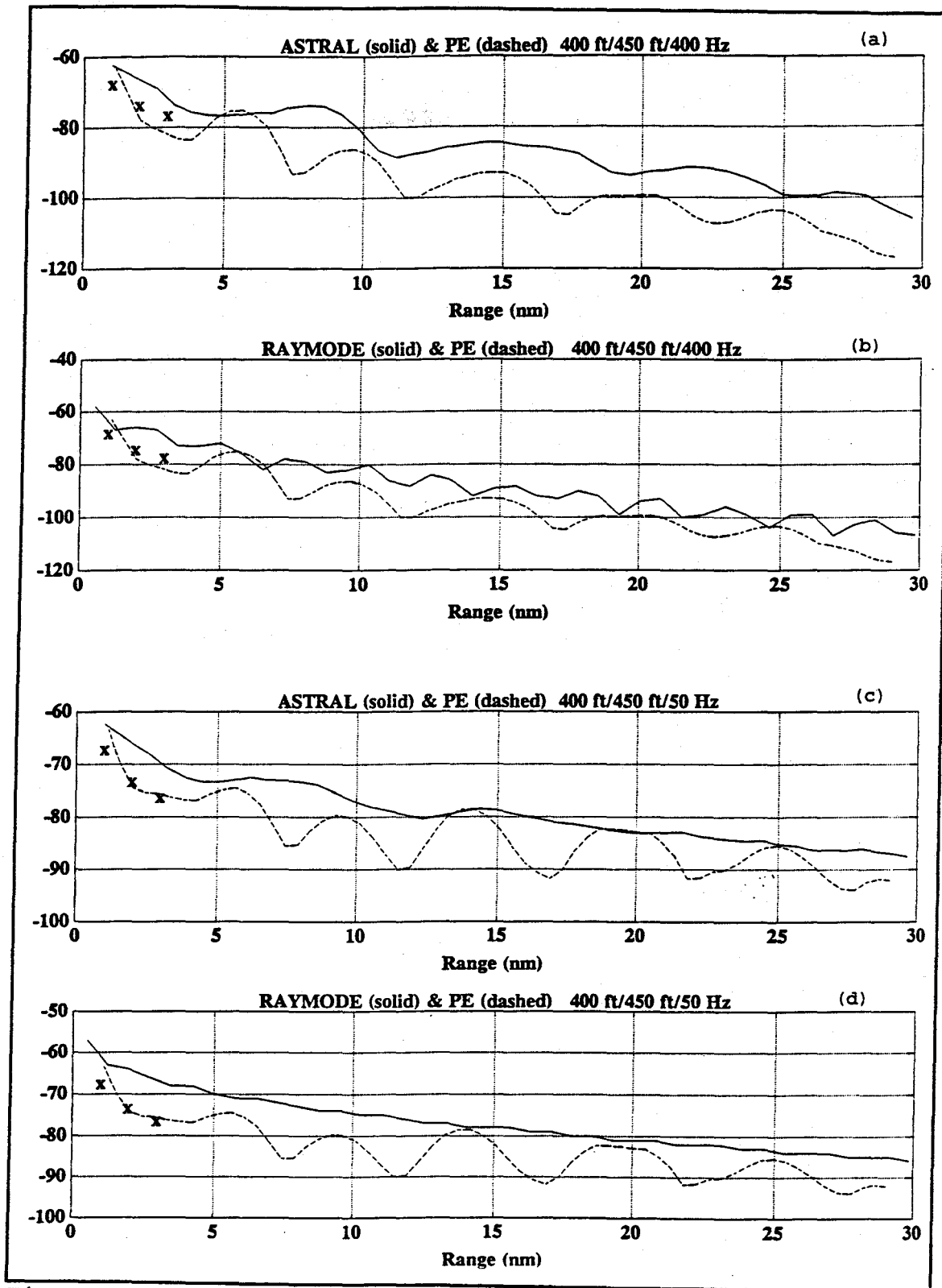


Figure 19 - Proploss for Area 3: 400ft/450ft/400 Hz (a and b), 400ft/450ft/50 Hz (c and d)

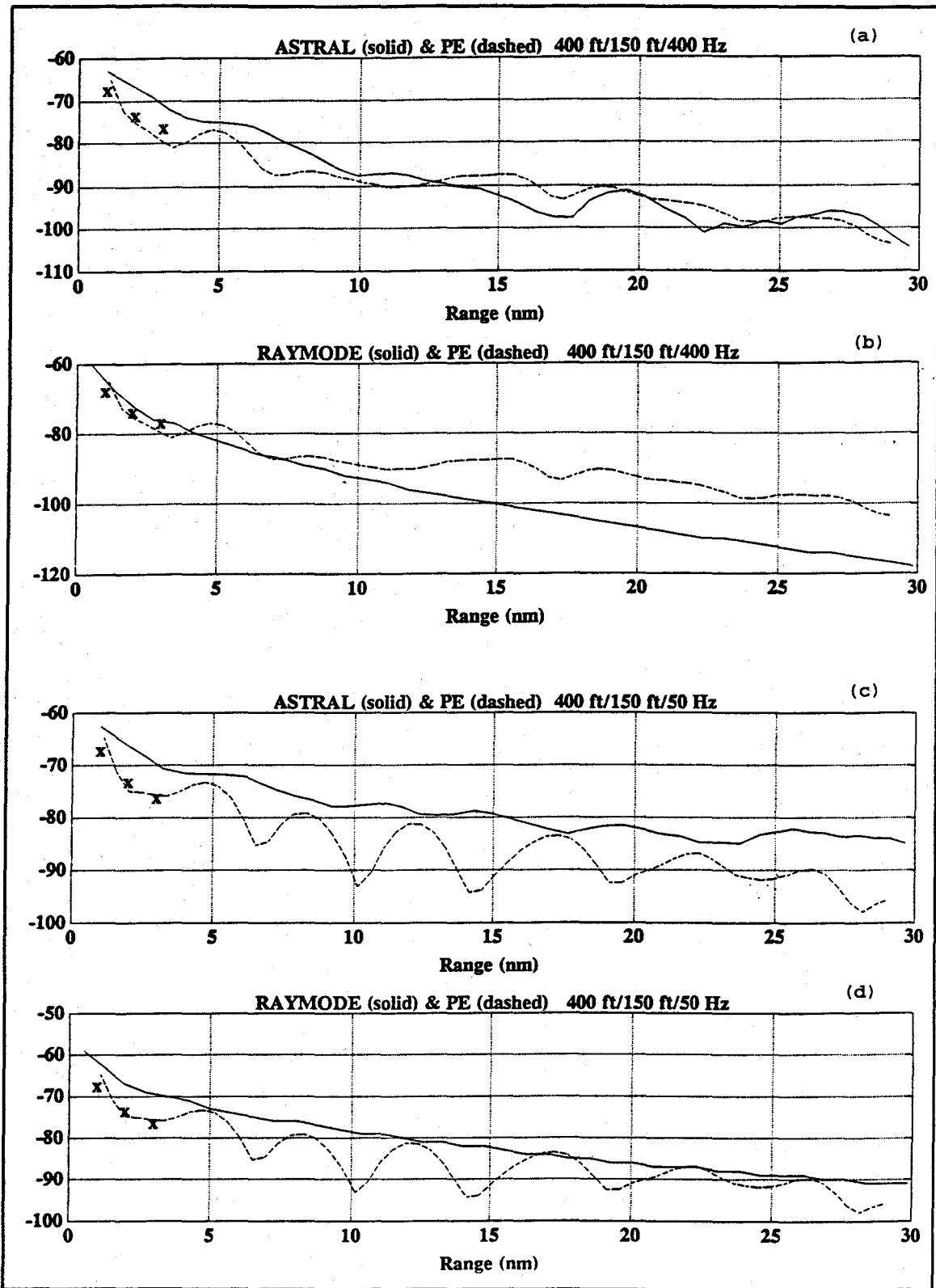


Figure 20 - Proploss for Area 3: 400ft/150ft/400 Hz (a and b), 400ft/150ft/50 Hz (c and d)

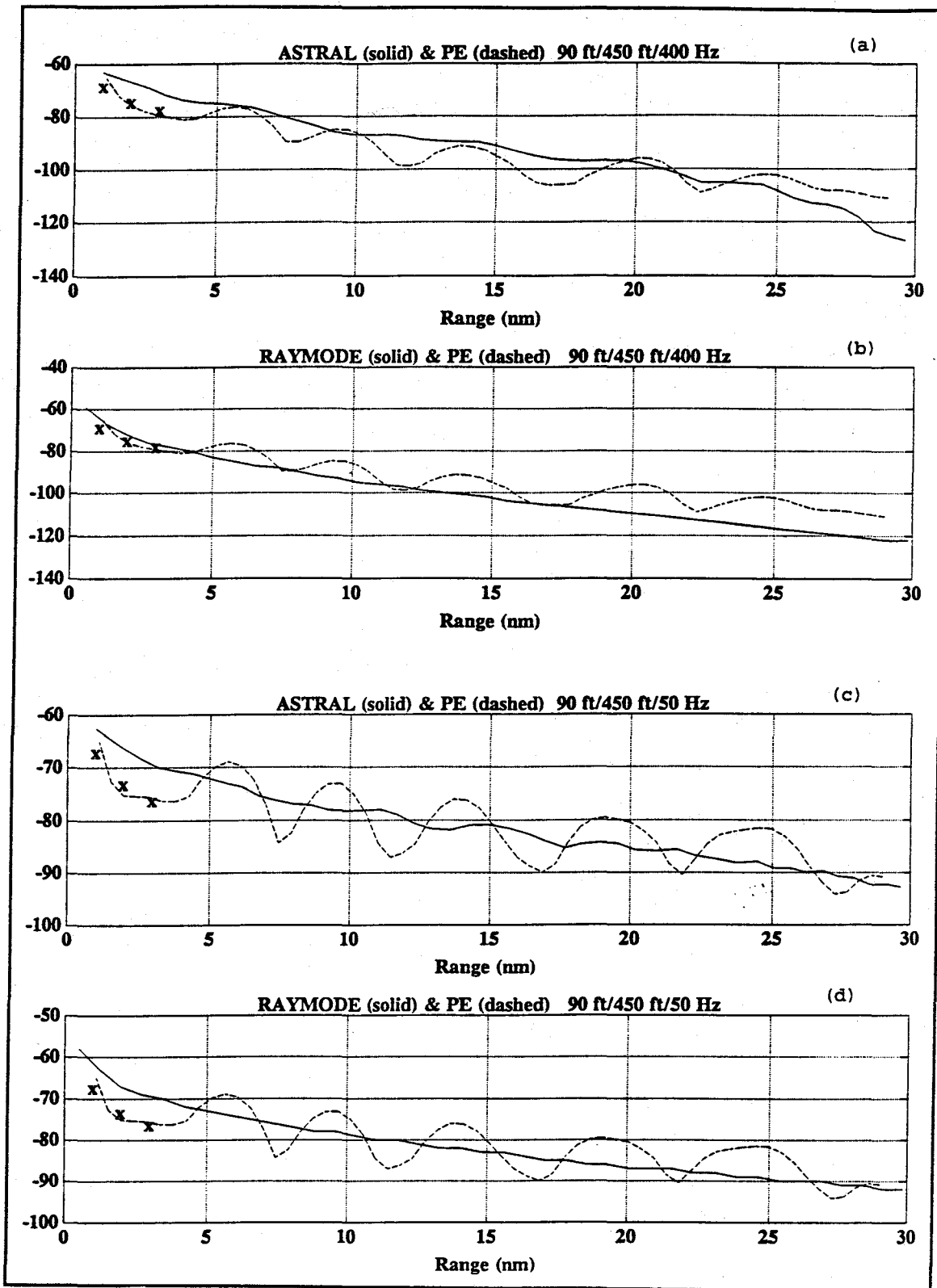


Figure 21 - Proploss for Area 3: 90ft/450ft/400 Hz (a and b), 90ft/450ft/50 Hz (c and d)

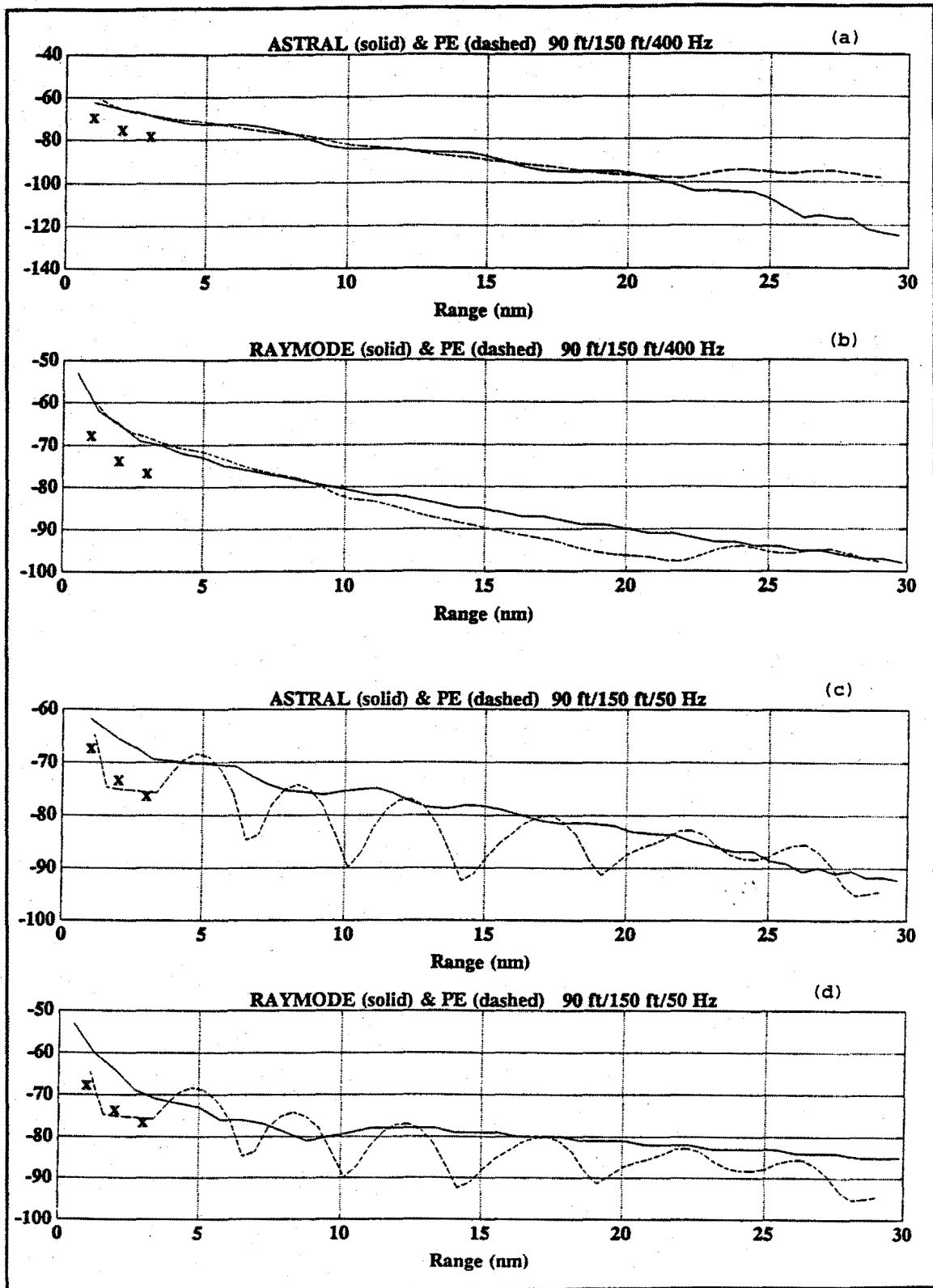


Figure 22 - Proploss for Area 3: 90ft/150ft/400 Hz (a and b), 90ft/150ft/50 Hz (c and d)

FOM 65			
Run	ASTRAL	PE	DIFF
A3MMH	6.0	2.5	3.5
A3MML	6.0	2.5	3.5
A3MSH	6.0	2.4	3.6
A3MSL	6.0	2.5	3.5
A3SMH	3.1	2.4	0.7
A3SML	4.3	2.4	1.9
A3SSH	6.2	6.2	0.0
A3SSL	6.2	2.5	3.7
Avg diff			2.6

FOM 65			
Run	RAY	PE	DIFF
A3MMH	2.5	2.5	0.0
A3MML	8.2	2.5	5.7
A3MSH	1.9	2.4	-0.5
A3MSL	4.3	2.5	1.8
A3SMH	2.4	2.4	0.0
A3SML	4.8	2.4	2.4
A3SSH	6.8	6.2	0.6
A3SSL	7.5	2.5	5.0
Avg diff			2.0

FOM 70			
Run	ASTRAL	PE	DIFF
A3MMH	12.9	4.3	8.6
A3MML	17.2	4.8	12.4
A3MSH	14.0	3.5	10.5
A3MSL	17.2	4.3	12.9
A3SMH	16.8	3.1	13.7
A3SML	17.3	3.1	14.2
A3SSH	23.3	24.8	-1.5
A3SSL	33.8	3.1	30.7
Avg diff			13.1

FOM 70			
Run	RAY	PE	DIFF
A3MMH	16.8	4.3	12.5
A3MML	42.1	4.8	37.3
A3MSH	4.3	3.5	0.8
A3MSL	21.1	4.3	16.8
A3SMH	4.8	3.1	1.7
A3SML	21.1	3.1	18.0
A3SSH	21.1	24.8	-3.7
A3SSL	16.8	3.1	13.7
Avg diff			13.1

FOM 75			
Run	ASTRAL	PE	DIFF
A3MMH	23.3	5.8	17.5
A3MML	98.1	9.6	88.5
A3MSH	33.8	6.2	27.6
A3MSL	87.8	10.7	77.1
A3SMH	27.8	6.2	21.6
A3SML	72.5	6.8	65.7
A3SSH	87.8	71.6	16.2
A3SSL	93.2	6.2	87.0
Avg diff			50.2

FOM 75			
Run	RAY	PE	DIFF
A3MMH	57.1	5.8	51.3
A3MML	99.7	9.6	90.1
A3MSH	8.2	6.2	2.0
A3MSL	71.6	10.7	60.9
A3SMH	11.1	6.2	4.9
A3SML	71.6	6.8	64.8
A3SSH	58.7	71.6	-12.9
A3SSL	55.7	6.2	49.5
Avg diff			42.1

FOM 80			
Run	ASTRAL	PE	DIFF
A3MMH	99.1	10.9	88.2
A3MML	100.0	75.4	24.6
A3MSH	89.9	55.7	34.2
A3MSL	100.0	60.1	39.9
A3SMH	87.8	73.2	14.6
A3SML	100.0	82.3	17.7
A3SSH	97.0	98.1	-1.1
A3SSL	100.0	65.3	34.7
Avg diff			31.9

FOM 80			
Run	RAY	PE	DIFF
A3MMH	94.1	10.9	83.2
A3MML	100.0	75.4	24.6
A3MSH	32.1	55.7	-23.6
A3MSL	100.0	60.1	39.9
A3SMH	32.1	73.2	-41.1
A3SML	100.0	82.3	17.7
A3SSH	97.8	98.1	-0.3
A3SSL	95.1	65.3	29.8
Avg diff			32.5

Figure 23 - Cumulative Detection Probability Comparisons (%)
 ASTRAL-PE (left) and RAYMODE-PE (right)

V. CONCLUSIONS

The ASTRAL propagation loss model consistently predicted much longer detection ranges than either the PE or RAYMODE models. This could lead to incorrectly spaced patterns and an overly optimistic probability of detection. RAYMODE generally predicted ranges consistent with or slightly shorter than PE. This would result in a more conservative search and provide a lower chance of allowing a target to slip through an area undetected. At lower figures of merit the difference between models is fairly small. However, at higher FOM's there are significant differences in transmission loss predictions.

No attempt was made to compare the ASTRAL or RAYMODE predictions with empirically gathered data, thus no conclusions as to which model better reflects reality is made.

With the current computer technology (ASQ 212 computer) being installed on ASW aircraft, processing capability and storage memory for new decision support systems are limited. Considering this limitation combined with the evolution of quieter submarines and shorter detection ranges, installing the more complex and computation intensive ASTRAL program may not be the best choice. The passive range independent RAYMODE propagation loss model, as shown in this report, will provide adequate transmission loss predictions.

LIST OF REFERENCES

1. Interview between Mort Metersky, Systems Engineer, Naval Air Warfare Center, and the author, 20 October 1993.
2. Medeiros, Robert C., *A Simplified Overview of the RAYMODE Propagation Loss Model*, p. 1, New England Technical Services, November 1985.
3. Officer, C. B., *Introduction to the Theory of Sound Transmission*, McGraw-Hill Book Company, New York, 1958.
4. Urick, Robert J., *Principles of Underwater Sound*, Third Edition, pp. 120-123, McGraw-Hill Book Company, 1983.
5. New England Technical Services, Document No. 8205, *RAYMODE Passive Propagation Loss Program Performance Specification*, by R.C. Medeiros, July 1982.
6. Naval Undersea Warfare Center, OAML-SDD-01B, *Software Design Document for the 1985 Baseline Passive RAYMODE Computer Program*, March 1993.
7. Naval Oceanographic Office, OAML-SRS-23D, *Software Requirements Specification for the ASTRAL Model (version 4.1)*, Science Applications International Corporation, February 1993.
8. NORDA Technical Note-346, *A Review of Candidate Shallow-Water Propagation Loss Models*, by Robert McGirr and David King, January 1989.
9. Sawrey, William M., *A Comparison of Propagation Loss Output from the Tactical Environmental Support System (TESS v.2.2a) and ASW Tactical Decision Aid (v.2.1.2.1)*, Master's Thesis, Naval Postgraduate School, Monterey, California, March 1993.
10. Rovero, P.J., LCDR USN, *Binary to ASCII Conversion Program*, December 1992.
11. Daniel H. Wagner, Associates, *The Effects of a Non-Homogeneous Environment on Passive Sonobuoy Search for a Submerged Target*, Appendix A and B, December 1988.

APPENDIX A

A. RUN IDENTIFICATION

Each propagation loss run was identified by a consistent code as follows: {A num B C D E}, where A represents Area, "num" is either 1, 2, or 3, B is the receiver depth (M=400ft, S=90ft), C is the source depth (M=450ft, S=150ft), D is the source frequency (H=400 Hz, L=50 Hz), and E is either RD, RI, or PE (RD=ASTRAL, RI=RAYMODE, PE=Parabolic Equation Model). For example A1MMHRD is a run in Area 1 with receiver at 400ft, source at 450ft, frequency of 400 Hz, and was run using ASTRAL.

B. ASWTDA DATA COLLECTION

Data from the ASWTDA PE and ASTRAL models was accessed after the propagation loss plot was generated. The system stored the current graph data in a file called OUTPUT.LOG in the exec/data/tactical directory for ASTRAL and in a file called for042.dat in the exec directory for PE. By opening a new window and changing to the necessary directory the files were copied to a new file. If this was not done the next graph created would overwrite the previous information. The ASTRAL data was in ASCII format and immediately available. The PE information was in a binary form and had to be converted via a Fortran program listed in Appendix B. The

RAYMODE data was not stored for retrieval as in ASTRAL or PE. Instead, using the "TDA", "Range Independent", "Proploss", "Info" selections from the menu bar, a tabular summary of RAYMODE range and propagation loss is displayed. By using the mouse and left button to highlight the vectors, then "vi" to open an editor in an open window, the center mouse button was used to copy the data to a new text file with the appropriate name. [Ref. 7]

The proploss files were edited and made into "m" files for the purpose of creating and analyzing the graphs using the Matlab program.

The following tables contain the predicted Median detection ranges from all three models at each of the four Figures of Merit (65, 70, 75, 80 dB).

ASTRAL

RUN/FOM	65	70	75	80
A1MMHRD	1.5	3.0	6.2	16.7
A1MMLRD	1.6	3.9	8.0	29.5
A1MSHRD	1.6	2.8	5.0	17.1
A1MSLRD	1.7	3.6	6.8	20.0
A1SMHRD	1.6	3.3	5.7	17.1
A1SMLRD	1.6	3.5	8.9	24.6
A1SSHRD	2.1	6.8	19.0	46.4
A1SSLRD	1.9	3.5	10.6	23.9

RAYMODE

RUN/FOM	65	70	75	80
A1MMHRI	1.0	1.7	3.5	11.0
A1MMLRI	1.1	1.8	4.3	16.5
A1MSHRI	1.2	1.6	2.3	7.3
A1MSLRI	1.2	1.5	5.0	15.7
A1SMHRI	0.9	1.6	2.3	7.3
A1SMLRI	0.9	1.5	2.0	15.7
A1SSHRI	1.2	2.8	8.8	20.0
A1SSLRI	1.0	1.1	3.5	15.5

PE

RUN/FOM	65	70	75	80
PEMMHRI	1.3	2.2	3.2	16.3
PEMMLRI	1.3	2.1	4.1	15.0
PEMSHRI	1.4	2.3	3.0	16.0
PEMSLRI	1.3	2.2	3.9	15.8
PESMHRI	1.2	2.3	3.1	15.6
PESMLRI	1.1	2.1	4.0	14.6
PESSHRI	2.3	7.0	20.6	30.0
PESSLRI	1.3	2.1	3.5	18.3

Table V - Area 1 Median Detection Ranges

ASTRAL

RUN/FOM	65	70	75	80
A2MMHRD	1.5	2.1	3.0	3.8
A2MMLRD	1.3	2.4	3.5	4.6
A2MSHRD	1.7	2.2	3.1	5.0
A2MSLRD	1.5	2.3	3.2	4.1
A2SMHRD	1.5	2.1	3.2	5.3
A2SMLRD	1.4	2.2	3.1	4.1
A2SSHRD	1.8	3.8	6.3	9.6
A2SSLRD	1.6	2.3	3.2	4.1

RAYMODE

RUN/FOM	65	70	75	80
A2MMHRI	0.7	1.3	1.5	2.0
A2MMLRI	1.1	1.4	1.8	2.3
A2MSHRI	0.6	1.0	1.6	2.0
A2MSLRI	0.7	1.0	1.6	1.9
A2SMHRI	0.7	1.0	1.4	1.8
A2SMLRI	0.7	1.0	1.4	1.8
A2SSHRI	1.4	2.7	6.5	14.0
A2SSLRI	2.1	2.8	5.0	5.4

PE

RUN/FOM	65	70	75	80
PEMMHRI	1.2	1.4	1.8	2.2
PEMMLRI	1.4	2.0	2.6	3.3
PEMSHRI	1.2	1.4	1.9	3.0
PEMSLRI	1.3	1.9	2.2	3.2
PESMHRI	1.3	1.9	2.2	3.2
PESMLRI	1.3	1.9	2.2	3.3
PESSHRI	1.9	3.8	6.7	11.5
PESSLRI	1.4	1.9	2.3	3.2

Table VI - Area 2 Median Detection Ranges

ASTRAL

RUN/FOM	65	70	75	80
A3MMHRD	1.8	2.7	3.7	9.7
A3MMLRD	1.8	3.2	9.0	16.2
A3MSHRD	1.8	2.8	4.4	7.5
A3MSLRD	1.8	3.2	7.3	15.2
A3SMHRD	1.3	3.0	5.0	7.3
A3SMLRD	1.5	3.2	6.6	12.2
A3SSHRD	1.9	3.7	7.3	8.6
A3SSLRD	1.9	4.4	7.8	16.3

RAYMODE

RUN/FOM	65	70	75	80
A3MMHRI	1.2	3.0	5.6	8.0
A3MMLRI	2.2	5.0	10.3	17.8
A3MSHRI	1.0	1.5	2.2	4.3
A3MSLRI	1.5	3.5	6.5	12.8
A3SMHRI	1.1	1.6	2.6	4.3
A3SMLRI	1.6	3.5	6.5	11.0
A3SSHRI	2.0	3.5	5.7	9.5
A3SSLRI	2.1	3.0	5.5	8.3

PE

RUN/FOM	65	70	75	80
PEMMHRI	1.2	1.5	1.8	2.5
PEMMLRI	1.2	1.6	2.3	6.8
PEMSHRI	1.1	1.4	1.9	5.7
PEMSLRI	1.1	1.5	2.4	6.0
PESMHRI	1.1	1.3	1.9	6.6
PESMLRI	1.1	1.3	2.0	7.0
PESSHRI	1.9	3.8	6.5	9.1
PESSLRI	1.2	1.3	1.9	6.2

Table VII - Area 3 Median Detection Ranges

APPENDIX 2

A. PE DATA CONVERSION

The following Fortran program was used to convert ASWTDA binary format (PE output) to ASCII output. Load into any directory and run by calling filename.[Ref. 8]

```
character*32 infile, outfile
character*9 when
integer*2 ititl(40),nr, nz,nprof, nbotm, nthb,nd
real      f,zs,xz(20),xr,thmin,thmax,thc,d1,d2
real      tthb(20),rthb(20),rplot,tl(20)
print *, 'Enter input file (for042.dat format) name:'
read(5,*)infile
open(unit=1,form='unformatted',status='old',file=infile)
print *, 'Enter output file name:'
read(5,*)outfile
open(unit=2,status='new',file=outfile)
c READ THE HEADER RECORD OF THE TL FILE
read(1)ititl,when,f,zs,nr,nz,(xz(i),i=1,nz)
c write out four lines of header information
print *,ititl
write(2,*)ititl
print *,when,f,zs,nr,nz,(xz(i),i=1,nz)
write(2,*)when,f,zs,nr,nz,(xz(i),i=1,nz)
print *, 'Range      TL'
write(2,*) 'Range      TL'
print *, '-----'
write(2,*) '-----'
nd=1
print *, 'Number of depths is',nd
c read the range and tl values, print them to screen and c
to the output file
do 33 j=1,400
  read(1,end=888,err=999)rplot,(tl(i),i=1,nd)
  write(2,*)rplot,tl(i),i=1,nd)
33 continue
888 print *, 'End of file on .042 file'
close(1)
close(2)
print *, 'Normal termination'
stop
999 close(1)
```

```
close(2)
print *, 'Abnormal termination'
stop
end
```

B. NESST

The program used to evaluate the Cumulative Detection Probabilities of the three patterns of interest was the NORDA Environmentally Sensitive Sonobuoy Tactics (NESST) program, provided by Wagner and Assoc. NESST has two main capabilities. First, the performance of an arbitrary sonobuoy pattern can be evaluated with respect to a user specified environment. Second, for a given environmental description of a region, NESST will develop a sonobuoy pattern which optimally searches that region. [Ref. 11]

Only the first of these two capabilities was used for this project. For each of the search regions a 2x8, 4x4, and 5x6x5 sonobuoy pattern was constructed for each FOM, using 1.5 times the MDR for sonobuoy spacing and 1.67 times MDR for row spacing. To evaluate the sonobuoy patterns NESST records the location of each buoy in the pattern in terms of grid coordinates. The NESST program used the environment created by ASWTDA for the 50 nm by 50 nm regions as the basis for the grid. The patterns were centered on the area of interest and evaluated for probability of detection based on the full 50 x 50 nm area. The sonobuoys were evaluated as cookie cutter detectors with the detection ranges predicted by the given

model for the grid location. When the full region of interest was 100 percent covered by the cookie cutter detectors, the pattern was assumed to have a 100 percent probability of detection.

C. CYCLIC EFFECT IN PE PROFILES

The cyclic appearance seen in the 50 Hz PE proploss profiles is due to bottom reflections. The PE model generates transmission loss information using a $\pm 20^\circ$ beamwidth. In areas where the sound speed profile is strongly negative, like in Area 2 and Area 3, this narrow beamwidth is refracted downward and reflected off the bottom as seen in Fig. 24. When the beamwidth is increased to $\pm 40^\circ$ (see Fig. 25) the cyclic effect disappears. Both the ASTRAL and RAYMODE models use the wider beamwidth for their calculations. This seems to indicate that in cases where there is a large amount of bottom interaction the PE model is less than ideal. Since the ranges examined in this report are generally less than 10 nm, the information presented was not affected by this cyclic effect.

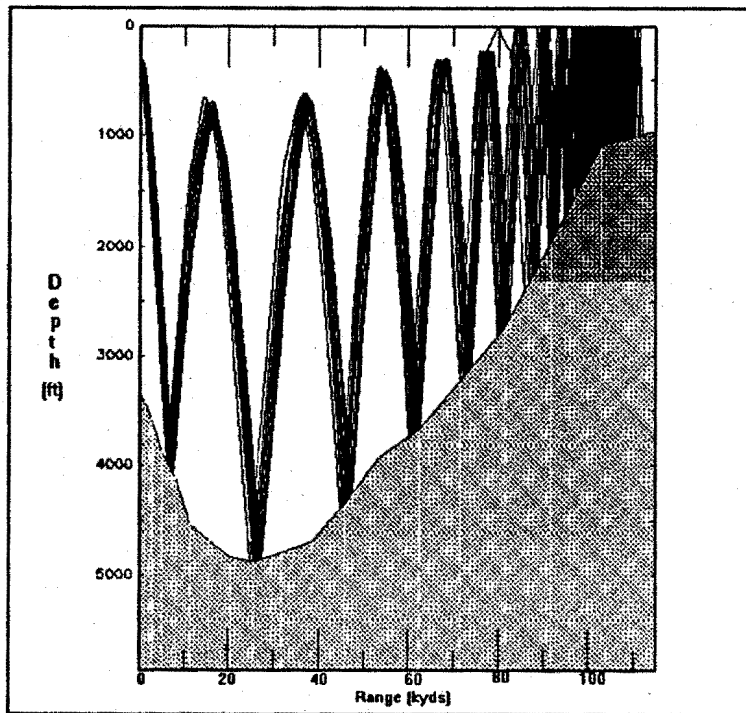


Figure 24 - Range Dependent Raytrace with Beamwidth of $\pm 20^\circ$

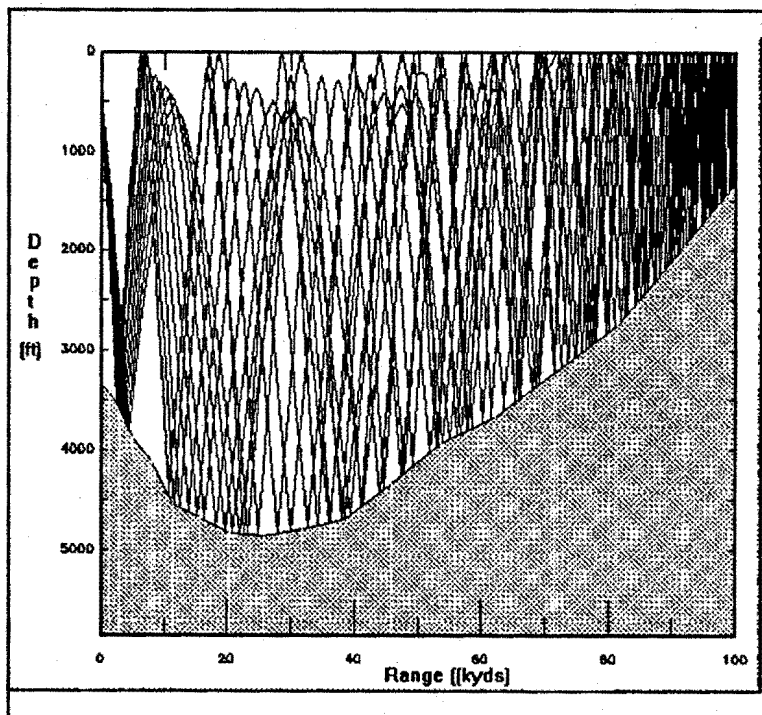


Figure 25 - Range Dependent Raytrace with Beamwidth of $\pm 40^\circ$

INITIAL DISTRIBUTION LIST

	No. Copies
1. Defense Technical Information Center Cameron Station Alexandria VA 22304-6145	2
2. Library, Code 052 Naval Postgraduate School Monterey CA 93943-5002	2
3. Director, Submarine Warfare Division (N87) Chief of Naval Operations Washington DC 20350-2000	
4. Department of the Navy Program Executive Officer for Air Warfare Washington DC 20362-5169	1
5. Commander, Naval Air Warfare Center Attention: Mr. Mort Metersky Warminster, PA 18974-5000	1
6. Alan B. Coppens, Code PH/CZ Physics Department Naval Postgraduate School Monterey CA 93943-5002	1
7. GPS Technologies Attention: Mr. Les Huff 9891 Broken Land Parkway, Suite 400 Columbia, MD 21046-1165	1
8. LT Michael T. Huff TSC Sigonella PSC 812 Box 3270 FPO AE 09627-3270	1

